Subgap modes in two-dimensional magnetic Josephson junctions

Yinan Fang

ynfang@ynu.edu.cn

Outline

I. Introduction

1. Superconductivity and the Josephson effect
2. Applications of the Josephson junctions

II. Two-dimensional magnetic Josephson junctions

1. Interplay of superconductivity and magnetic orders
2. Superconducting spintronics
3. Beyond one-dimensional junctions

III. Transverse subgap modes

1. The model
2. Flat-dispersion
3. Domain walls and applications

IV. 0 - π transitions in two-dimensional junctions

1. The Josephson current
2. Implications in experiments

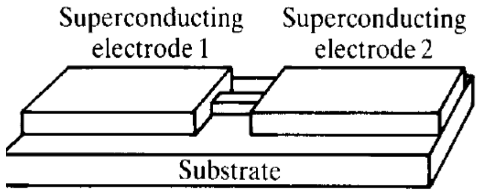

Tinkham 1996

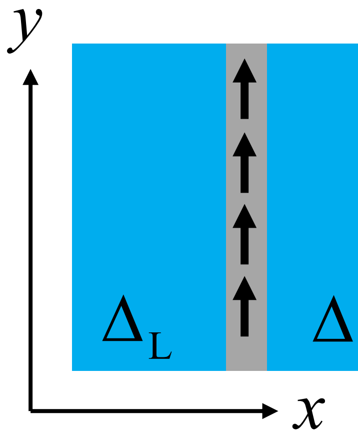

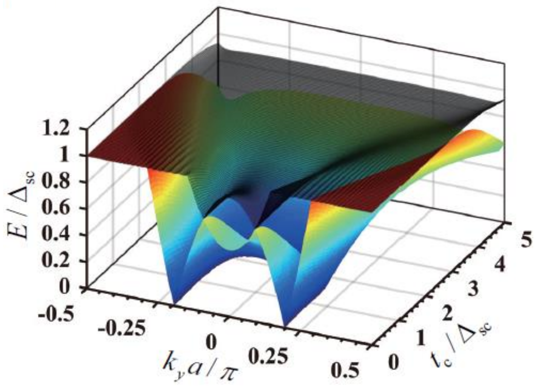

Y. Fang, S. Han, S. Chesi, and M.-S. Choi, Phys. Rev. B **107**, 115114 (2023)

Superconductivity and the Josephson effect

After Onnes successfully liquefied helium in 1908, the behavior of a sudden drop in resistivity of Hg below 4.2K was discovered in 1911

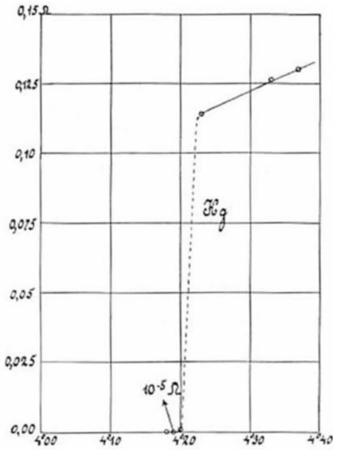

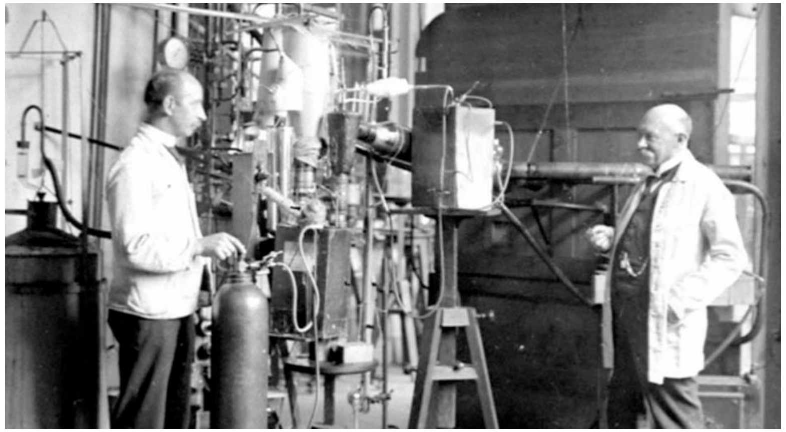

H. K. Onnes

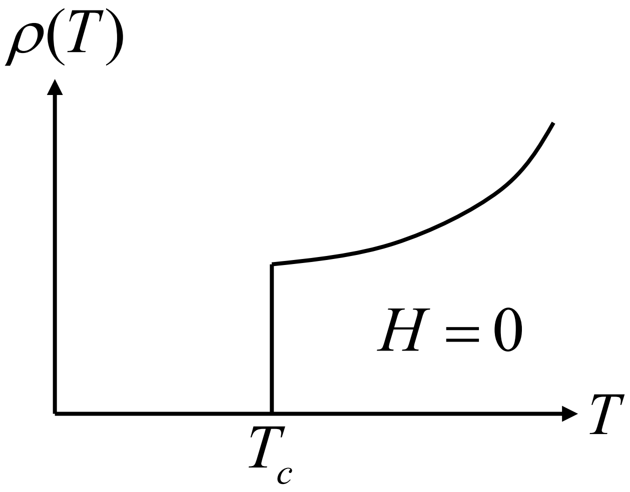

Meissner first observed complete diamagnetism in 1933

F. W. Meissner

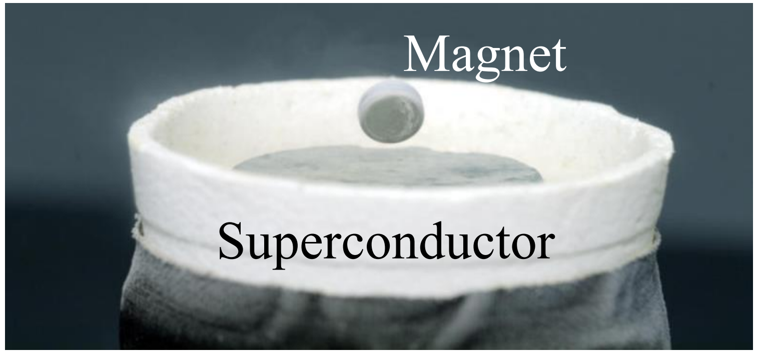

The Meissner effect

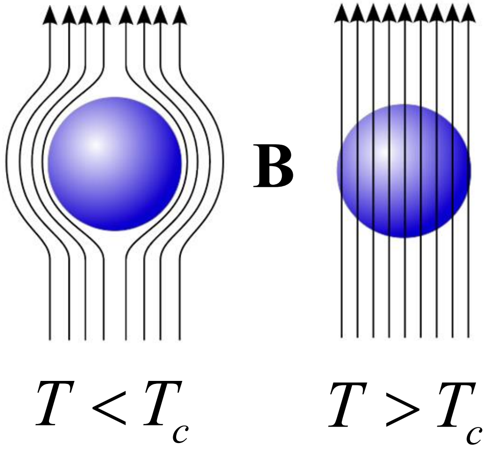

In 1957, the BCS theory proposed by Bardeen, Cooper, and Schrieffer successfully explained a series of physical phenomena that accompany the superconducting transition

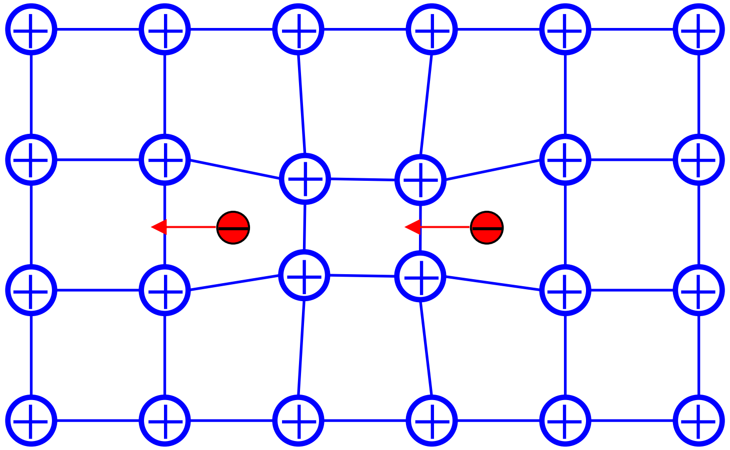

Electron-electron attraction induced by the electron-phonon interaction

$$\hat{H}' = -V \sum_{k,k'} \hat{c}^\dagger_{k'\uparrow} \hat{c}^\dagger_{-k'\downarrow} \hat{c}_{-k\downarrow} \hat{c}_{k\uparrow}$$

pairing potential $\Delta = V \sum_k \langle \hat{c}_{-k\downarrow} \hat{c}_{k\uparrow} \rangle$

$$\hat{H} = \sum_k (\varepsilon_k - \mu)\left(\hat{c}^\dagger_{k\uparrow}\hat{c}_{k\uparrow} + \hat{c}^\dagger_{-k\downarrow}\hat{c}_{-k\downarrow}\right) - \left(\Delta \hat{c}^\dagger_{k\uparrow}\hat{c}^\dagger_{-k\downarrow} + \text{h.c.}\right)$$

BCS Hamiltonian

$$|\text{BCS}\rangle = \prod_{k>0}\left(u_k + v_k e^{i\varphi} \hat{c}^\dagger_{k\uparrow}\hat{c}^\dagger_{-k\downarrow}\right)|0\rangle$$

$\Delta = |\Delta| e^{i\varphi}$ order parameter

BCS ground state wavefunction

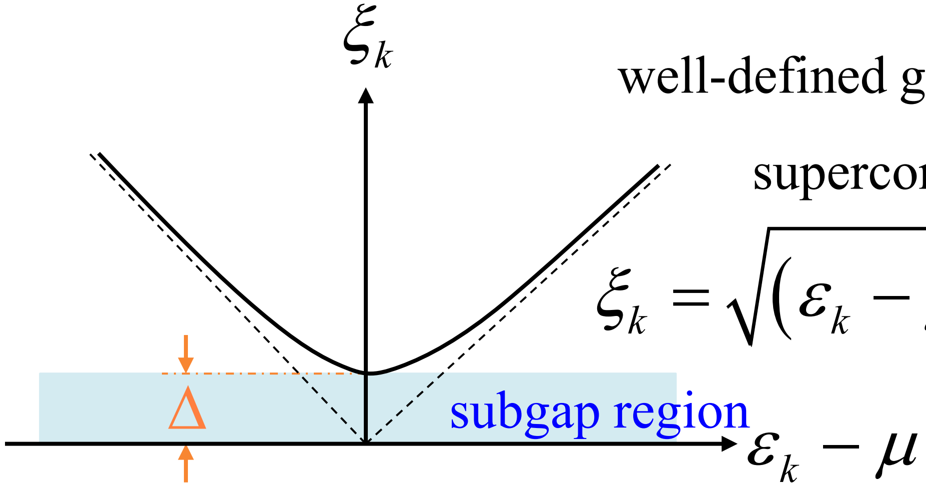

well-defined gap for s-wave superconductor

$$\xi_k = \sqrt{(\varepsilon_k - \mu)^2 + |\Delta|^2}$$

The Josephson effect was theoretically predicted by Brian D. Josephson from the University of Cambridge in 1962. Due to this discovery, he was awarded the Nobel Prize in Physics in 1973, along with Esaki of IBM and Giaever of the general electric company

- *For his theoretical predictions of the properties of a supercurrent through a tunnel barrier, in particular those phenomena which are generally known as the Josephson effects*

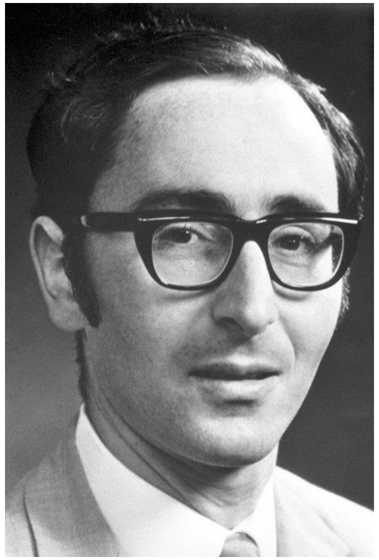

B. D. Josephson

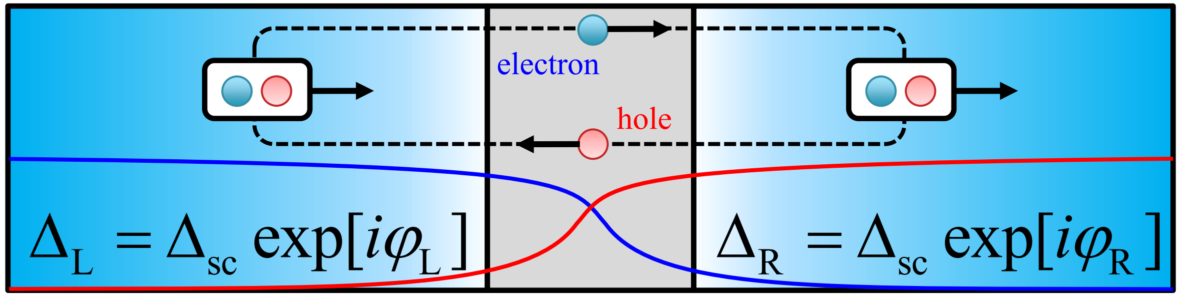

Superconductor 1 Normal metal Superconductor 2

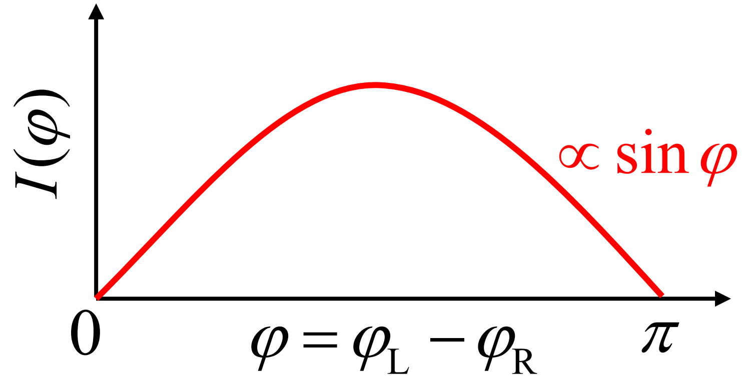

Current-phase relation (d.c.)

The current-phase relationship of Josephson current can be explained using the Cooper pair tunneling model

$$\hat{H}_L = \sum_k (\varepsilon_k - \mu)\left(\hat{c}^\dagger_{k\uparrow}\hat{c}_{k\uparrow} + \hat{c}^\dagger_{-k\downarrow}\hat{c}_{-k\downarrow}\right) - \left(\Delta_\mathrm{L}\hat{c}^\dagger_{k\uparrow}\hat{c}^\dagger_{-k\downarrow} + \mathrm{h.c.}\right)$$

$$\hat{H}_R = \sum_q (\varepsilon_q - \mu)\left(\hat{c}^\dagger_{q\uparrow}\hat{c}_{q\uparrow} + \hat{c}^\dagger_{-q\downarrow}\hat{c}_{-q\downarrow}\right) - \left(\Delta_\mathrm{R}\hat{c}^\dagger_{q\uparrow}\hat{c}^\dagger_{-q\downarrow} + \mathrm{h.c.}\right)$$

$$\hat{H}_T = t\sum_{k,q} \hat{c}^\dagger_{k\uparrow}\hat{c}^\dagger_{-k\downarrow}\hat{c}_{-q\downarrow}\hat{c}_{q\uparrow} + \mathrm{h.c.}$$

Effective 2nd order process

(Cooper pair tunneling)

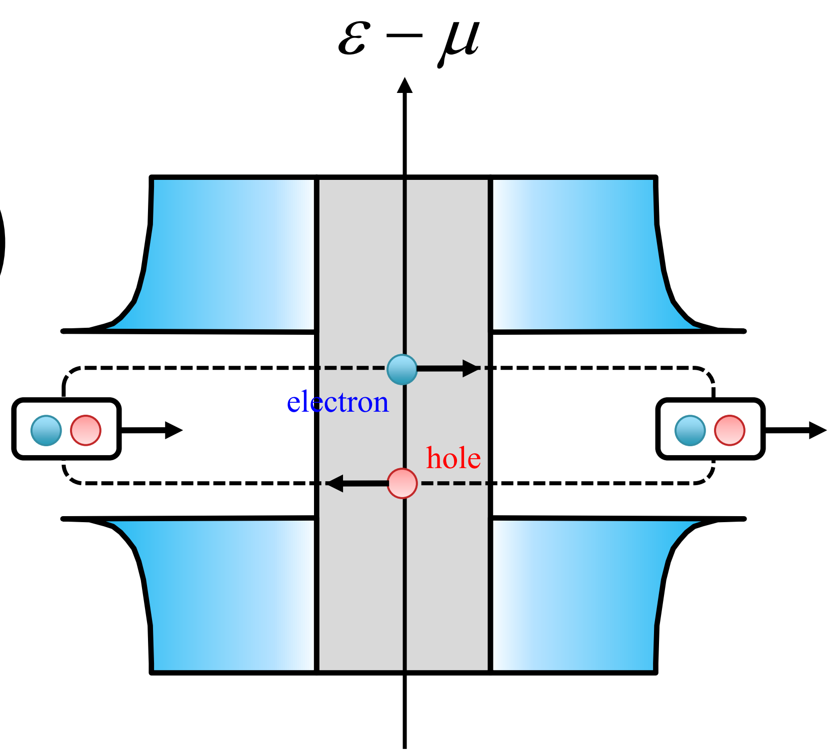

$$I \propto \langle \Psi_\mathrm{L} | \otimes \langle \Psi_\mathrm{R} | \frac{d}{dt}\hat{n}_\mathrm{L}(t) | \Psi_\mathrm{L}\rangle \otimes | \Psi_\mathrm{R}\rangle$$

$$= 4t\sum_{k,q} u_k v_k u_q v_q \sin\left(\varphi_\mathrm{L} - \varphi_\mathrm{R}\right) = I_c \sin\varphi$$

Physically, the current in the SNS Josephson junction can be regarded as being induced by Cooper pairs mediated by Andreev bound states

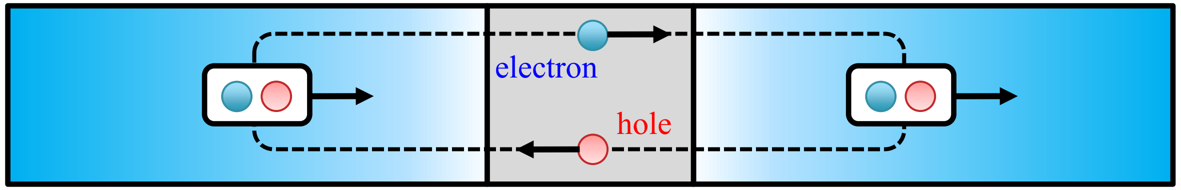

$$I = 2ev_g \qquad v_g = \frac{1}{\hbar}\frac{\partial E}{\partial k}$$

$$\left.\begin{array}{l}[\hat{n},\hat{\varphi}] = i \\ [\hat{x},\hat{p}] = i\hbar\end{array}\right\} \varphi \leftrightarrow k \Rightarrow I = \frac{2e}{\hbar}\frac{\partial E}{\partial \varphi}$$

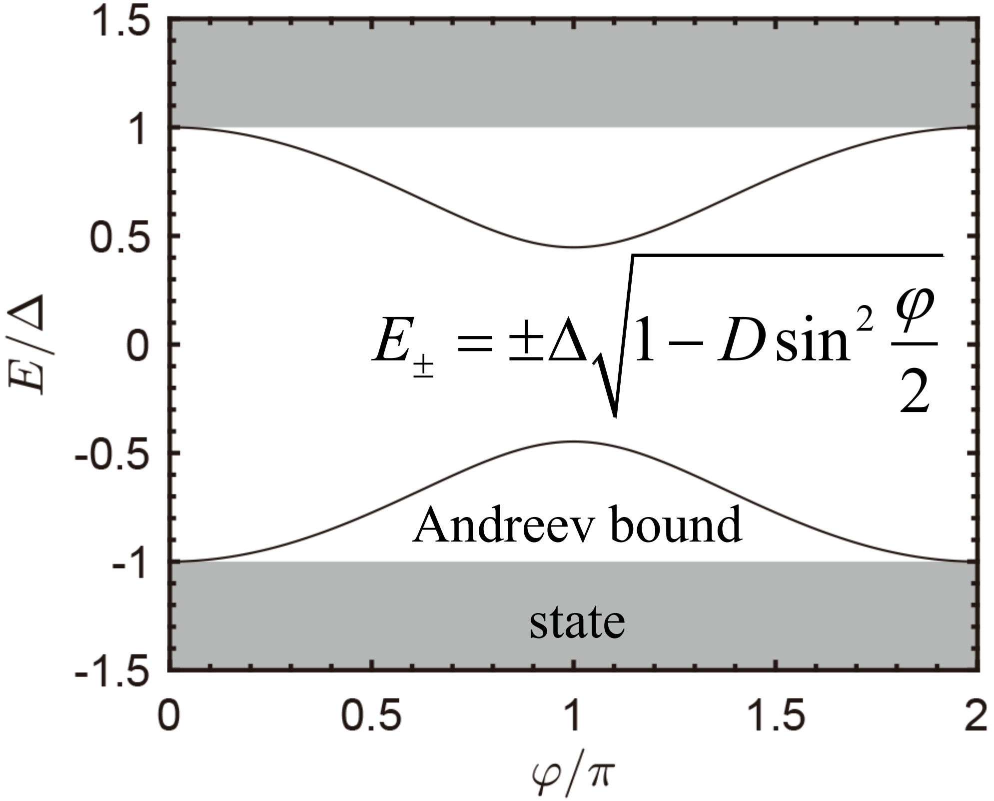

Subgap mode: In superconducting systems, a quasiparticle state with energy lower than the superconducting gap Δ, whose energy is related to the superconducting phase difference

The sub-gap modes are important for the behavior of the Josephson current $I = \frac{2e}{\hbar}\frac{\partial E_-}{\partial \varphi} \approx \frac{De\Delta}{2\hbar}\sin\varphi$

Applications of the Josephson junctions: Sensing of weak signals

The **flux quantization** in hollow superconductor and the **Josephson tunneling** are the physical principals of the Superconducting Quantum Interference Device (SQUID)

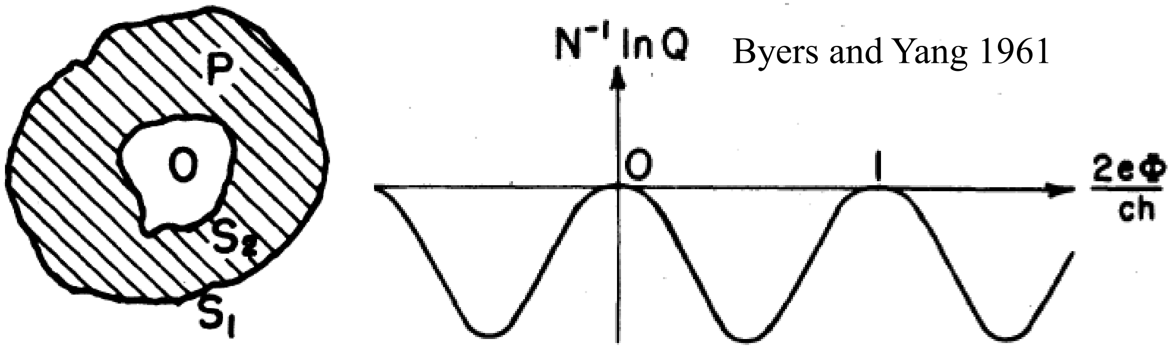

Byers and Yang 1961

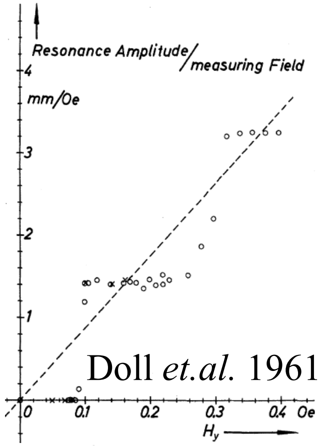

Doll *et.al.* 1961

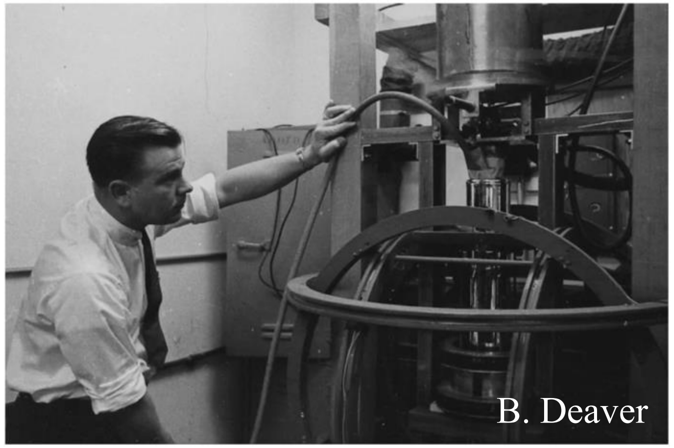

B. Deaver

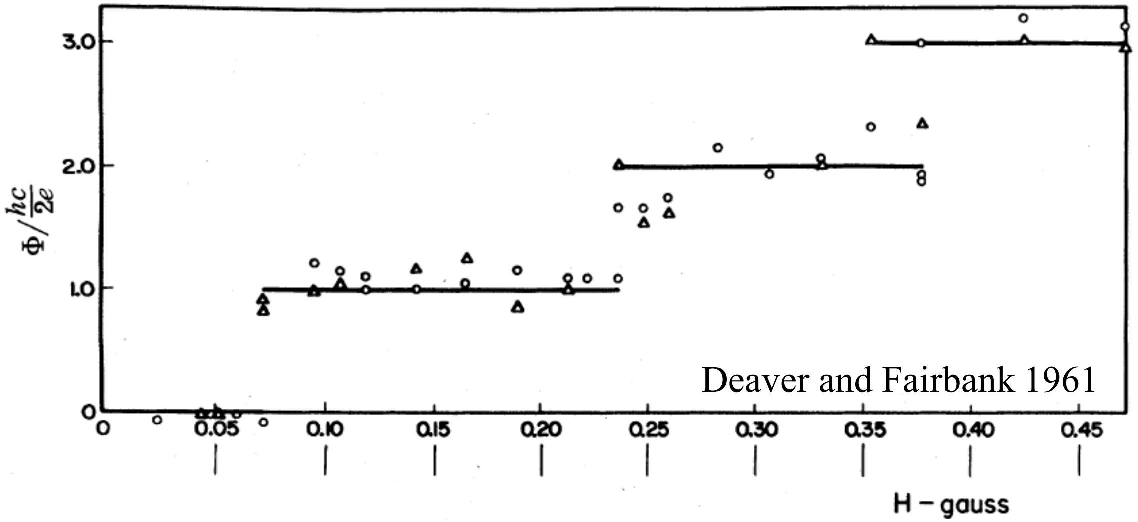

Deaver and Fairbank 1961

Equilibrium states reached at the maxima

Pairing of electrons forming Cooper pair

$$\psi' = \psi \exp\left[\sum_j i \frac{e}{\hbar c}\chi_j\right] \quad \psi' \to \psi' \exp\left[i\frac{e}{\hbar c}\Phi\right]$$

$$\Phi_0 = \frac{h}{2e} \approx 2.07\times10^{-15}\,\mathrm{Wb}$$

Utilizing the flux quantization and Josephson tunneling, quantum interference in SQUID provides sensitivity detection of weak signals

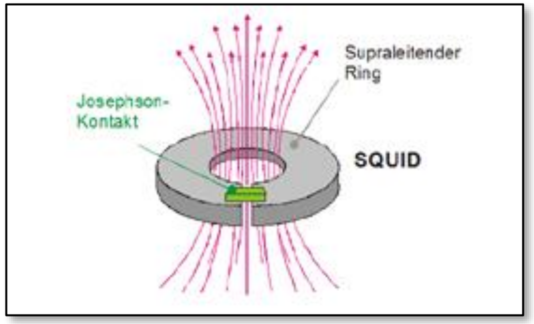

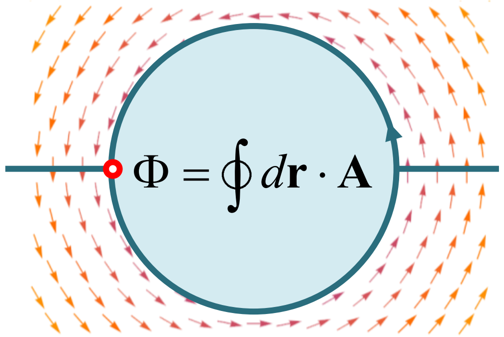

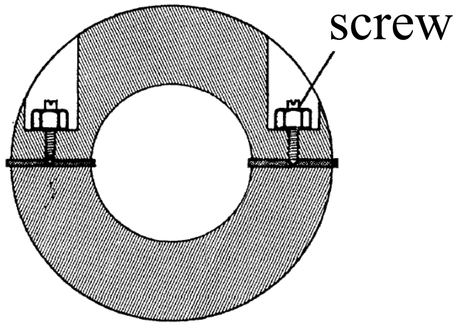

Zimerman and Silver 1961

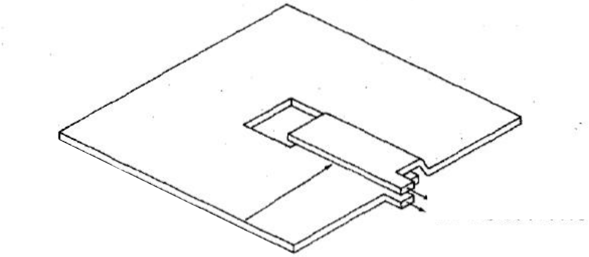

Ketchen *et.al.* 1981

Phase differences across two Josephson junctions

$$\gamma_1 - \gamma_2 = 2\pi \frac{\Phi}{\Phi_0}$$

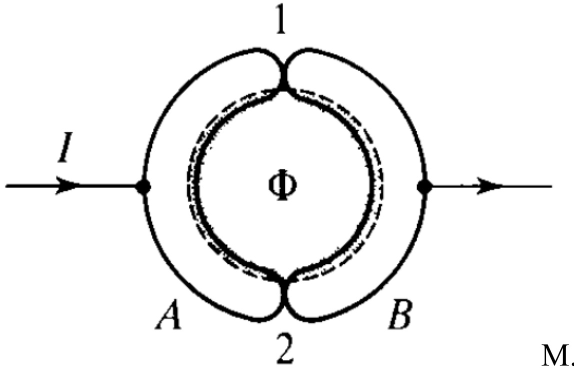

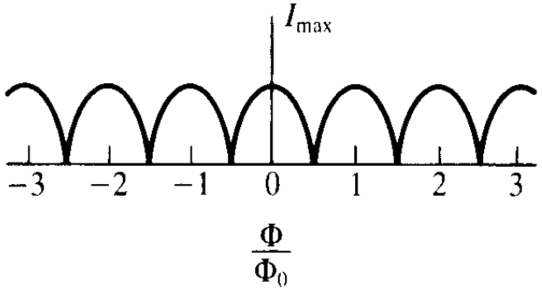

M. Tinkham, *Introduction to Superconductivity*

$$I = I_c \cos\frac{\pi\Phi}{\Phi_0} \sin\tilde{\varphi}$$

$$\Phi_0 = \frac{h}{2e} \approx 2.07 \times 10^{-15}\,\mathrm{Wb}$$

Various SQUID devices had been invented since the observation of quantum interference, with improving device robustness, tunable features, and integration

Films

Jaklevic *et.al.*, Phys. Rev. Lett. **7**, 159 (1964)

Point contact junction

Zimmerman and Silver, Phys. Rev. **141**, 367 (1966)

Superconducting low-inductance undulatory galvanometer

Clarke, Phil. Mag. **13**, 115 (1966)

Cylindrical dc SQUID

Clarke *et.al.*, J. Low Temp. Phys. **27**, 301 (1976)

Planar SQUID

Voss *et.al.*, J. Appl. Phys. 51, 2306 (1980); Ketchen *et.al.*, IEEE Trans. Magn. MAG-17, 400 (1981)

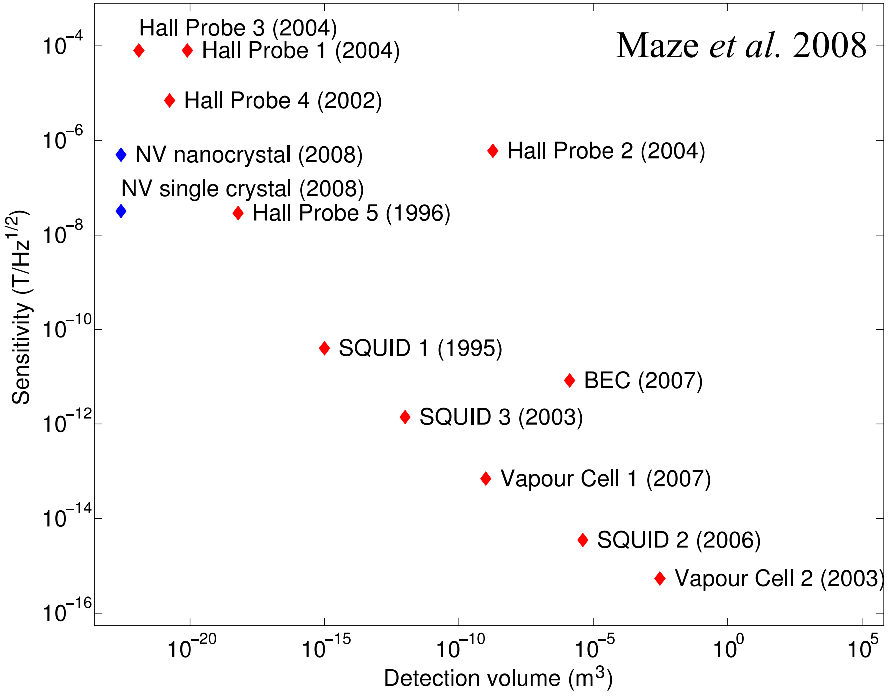

High T$_c$ SQUID Koch *et.al.*, Appl. Phys. Lett. 51, 200 (1987)

Applications of the Josephson junctions: Constructing qubits

Constructing qubits using Josephson structures (physical systems with two mutually orthogonal quantum states)

Initialization

Control

Readout

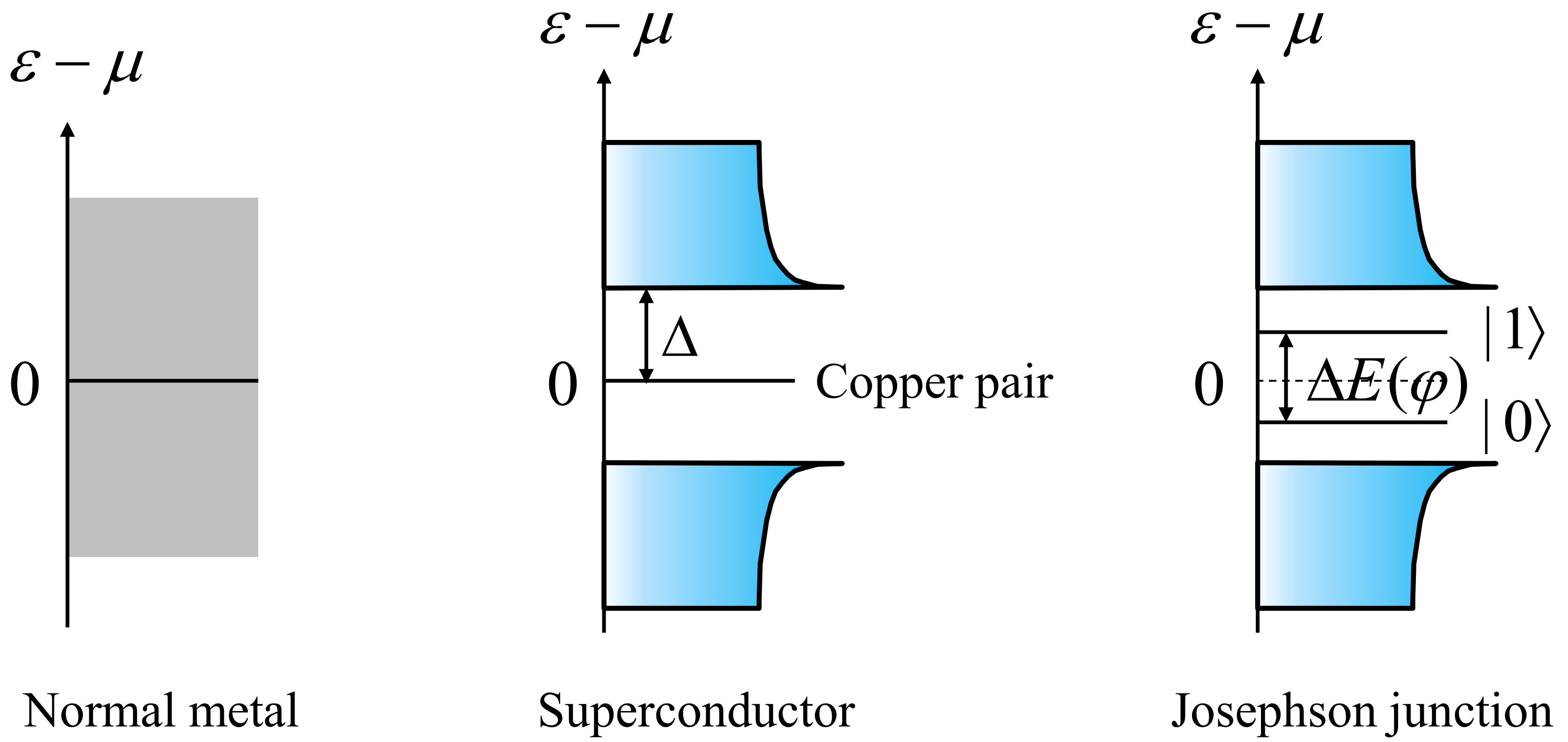

Superconducting charge qubit: competition between the charging energy and Josephson tunneling leads to energy splitting thus defines a qubit

$C_J \leq 10^{-15}\,\mathrm{F}$

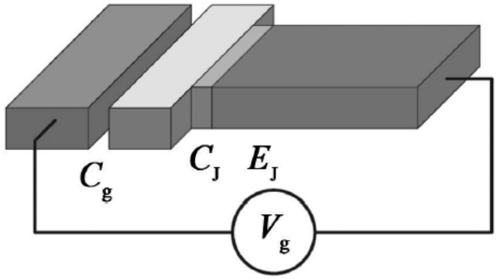

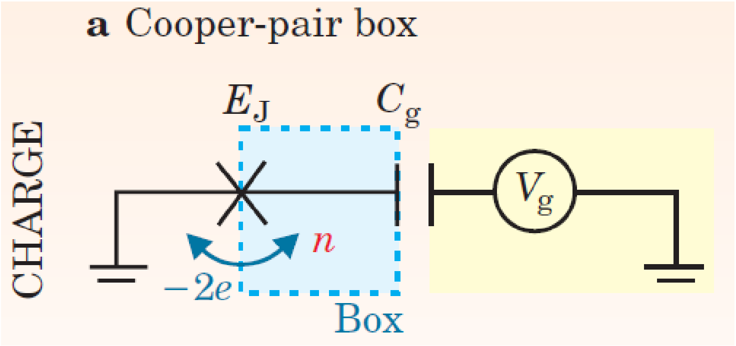

You *et al.* 2005

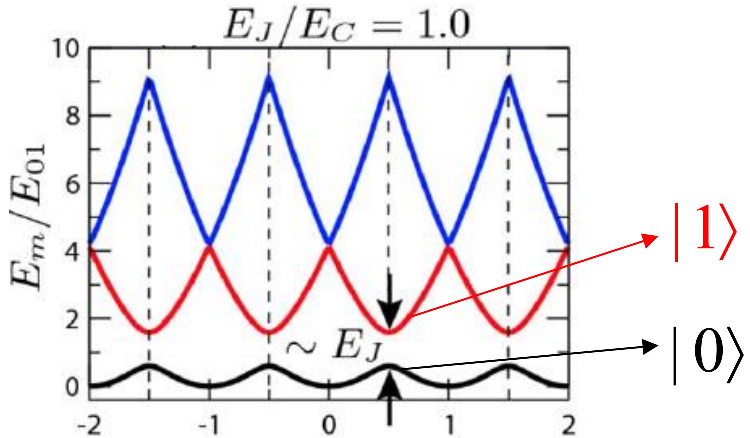

Koch *et.al.* 2007

$$E_C\left(\hat{n}-n_g\right)^2$$

$$\left.\begin{aligned} I &= \frac{2e}{\hbar}\frac{\partial E}{\partial k} \\ I &= I_c \sin\varphi \end{aligned}\right\} \quad -E_J\cos\varphi$$

$$E_C \approx 10E_J$$

High speed operation

Easy control and readout

Flexible device design

Sensitive to charge noise

Short coherence time

Superconducting transmon qubit: By connecting a large capacitor in parallel across the DC-SQUID junction, the qubit energy levels remain unchanged with gate voltage, reducing decoherence effects caused by charge noise at the cost of sacrificing anharmonicity

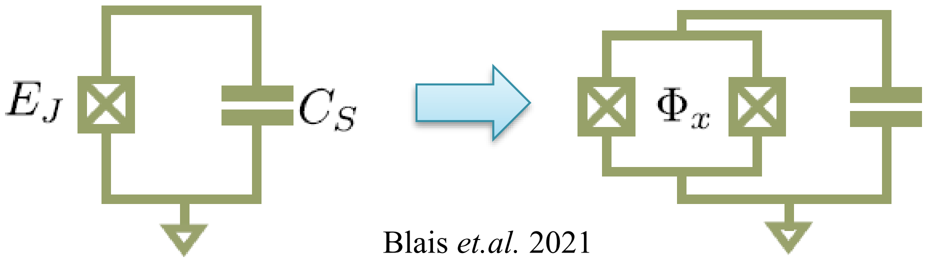

Blais *et.al.* 2021

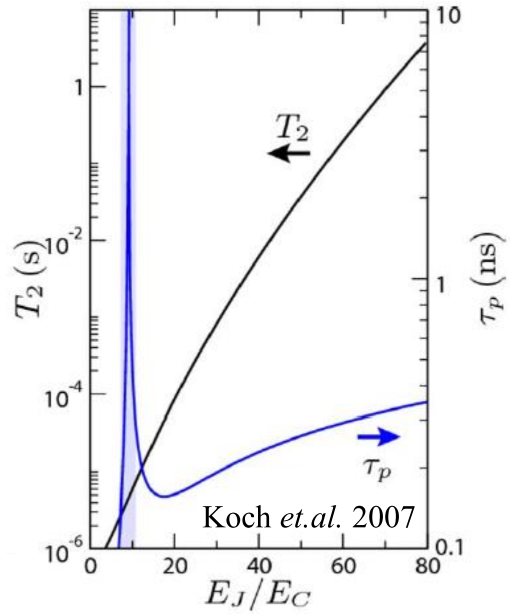

Koch *et.al.* 2007

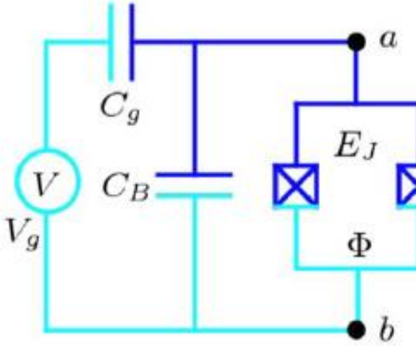

Koch *et.al.* 2007

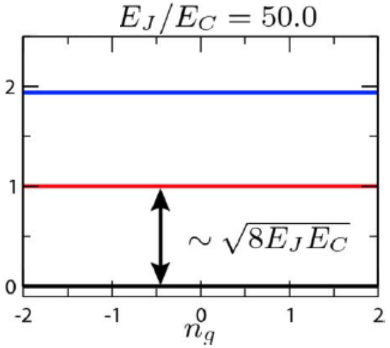

$$E_J / E_C \approx 50$$

Insensitive to charge noise

Longer coherence time

Weak anharmonicity

Minimizing the qubit size

Outline

I. Introduction

1. Superconductivity and the Josephson effect
2. Applications of the Josephson junctions

II. Two-dimensional magnetic Josephson junctions

1. Interplay of superconductivity and magnetic orders
2. Superconducting spintronics
3. Beyond one-dimensional junctions

III. Transverse subgap modes

1. The model
2. Flat-dispersion
3. Domain walls and applications

IV. $0-\pi$ transitions in two-dimensional junctions

1. The Josephson current
2. Implications in experiments

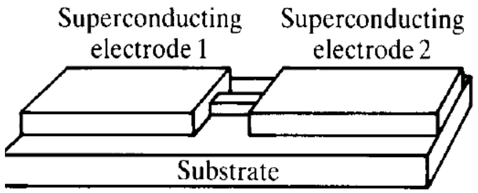

Tinkham 1996

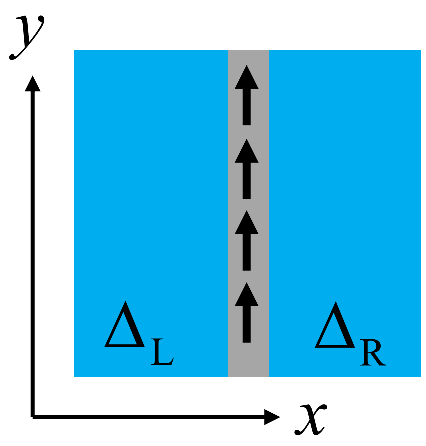

Interplay of superconductivity and magnetic orders

The interaction between superconducting order and ferromagnetic order can give rise to a wealth of physical phenomena

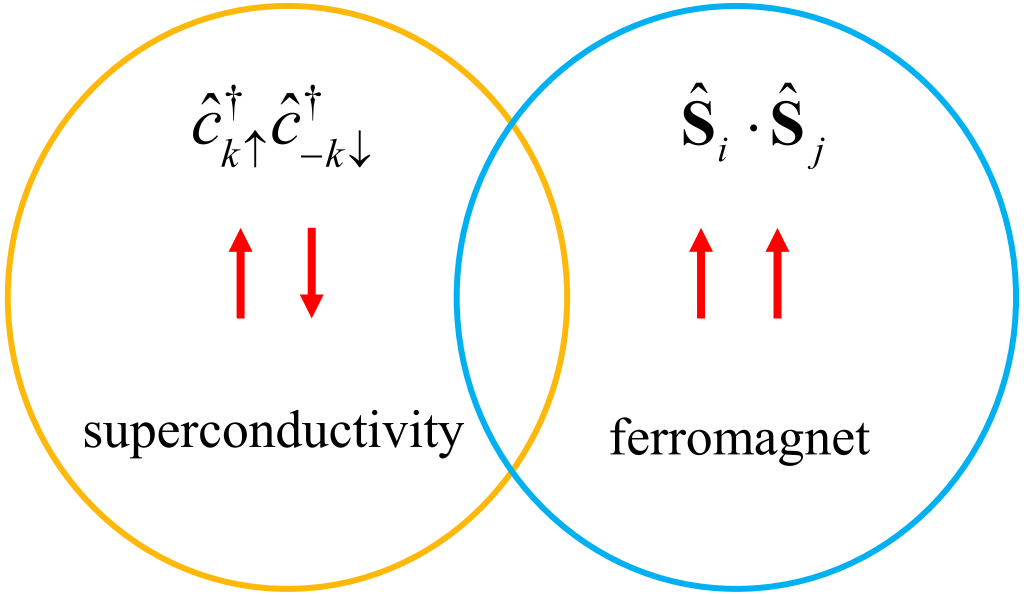

(Fulde-Ferrell-Larkin-Ovchinnikov)

FFLO pairing

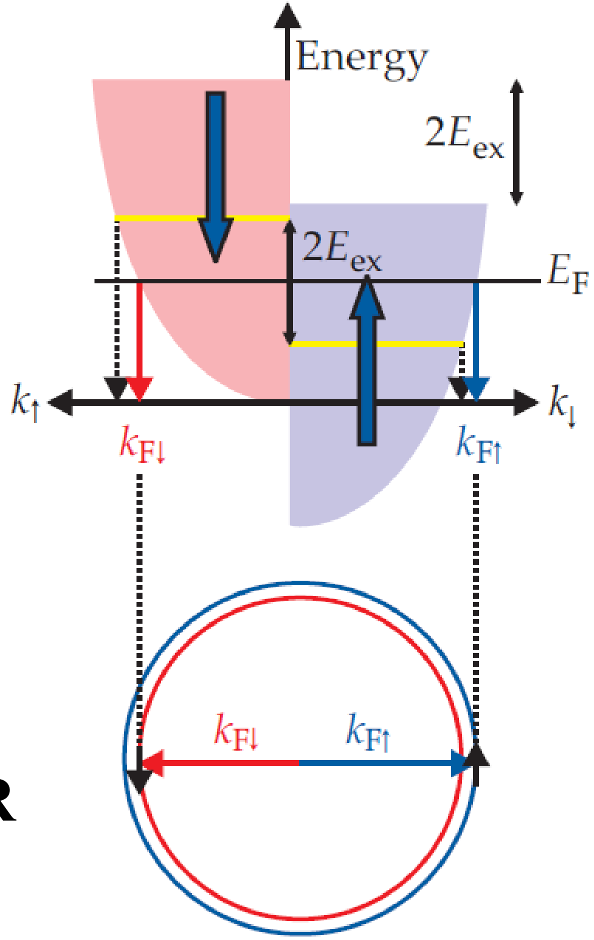

Eschrig 2011

$$\left(|\uparrow\downarrow\rangle - |\downarrow\uparrow\rangle\right)\cos \mathbf{Q}\cdot\mathbf{R}$$

$$|\uparrow\downarrow\rangle - |\downarrow\uparrow\rangle \qquad e^{i\mathbf{Q}\cdot\mathbf{R}}\,|\uparrow\downarrow\rangle - e^{-i\mathbf{Q}\cdot\mathbf{R}}\,|\downarrow\uparrow\rangle$$

$$\left(|\uparrow\downarrow\rangle + |\downarrow\uparrow\rangle\right)\sin \mathbf{Q}\cdot\mathbf{R}$$

Depending on the ferromagnet thickness (or spin-splitting), the ground state of the S/F/S junction has energy minimal either at $\varphi = 0$ or $\varphi = \pi$

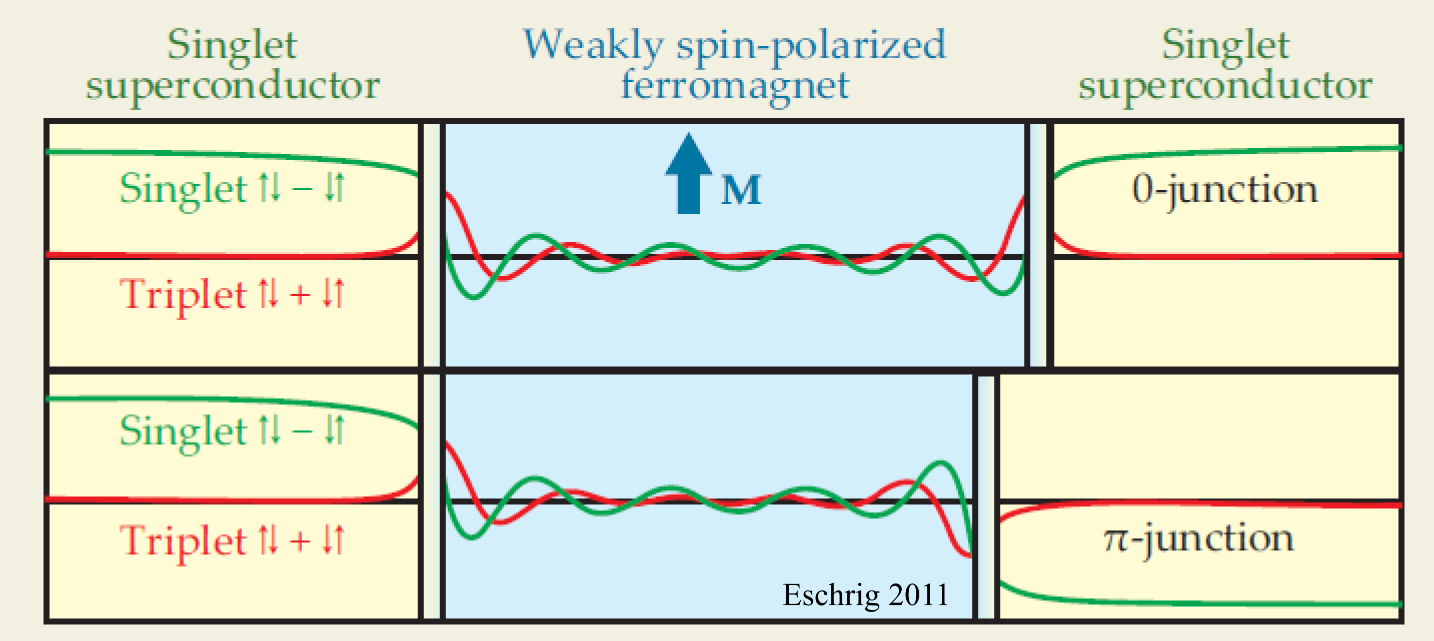

$$\left(|\uparrow\downarrow\rangle - |\downarrow\uparrow\rangle\right)\cos \mathbf{Q}\cdot\mathbf{R}$$

spin-splitting barrier thickness

0 - junction

equal superconducting phase

π - junction

opposite superconducting phase

$$\varphi \to \varphi + \pi$$

From the perspective of subgap mode, the 0 - π transition accompanied with a change of the highest occupied state with its energy minimal changing from $\varphi = 0$ to $\varphi = \pi$

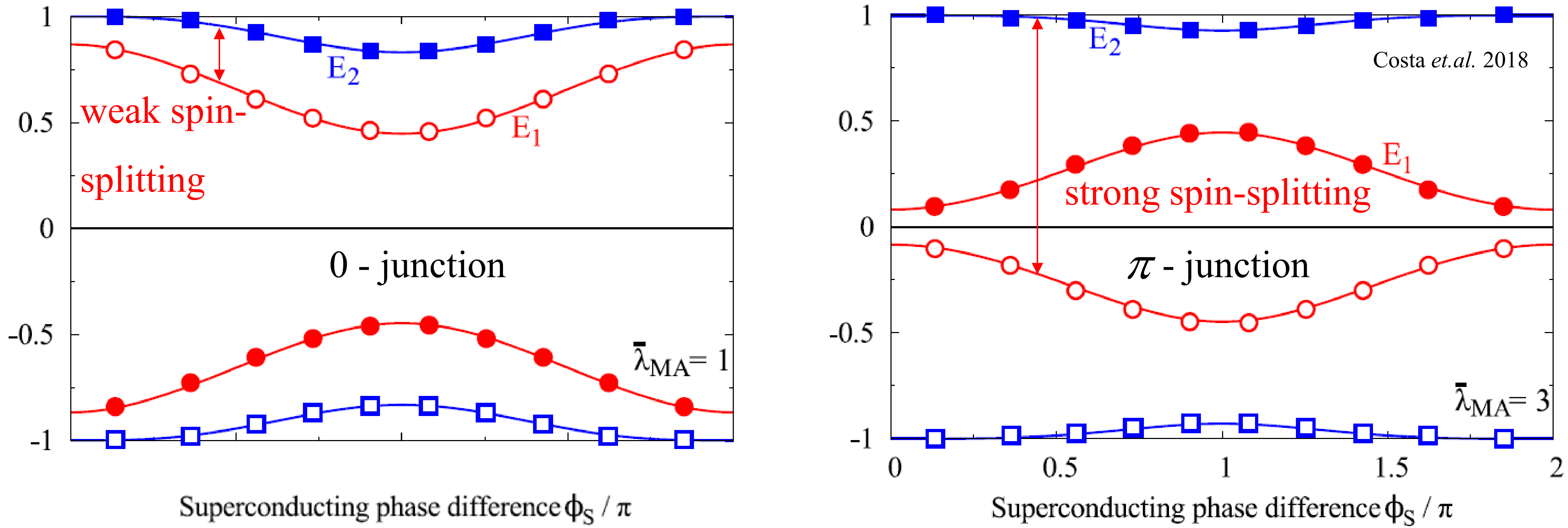

The additional phase difference $\varphi \to \varphi + \pi$ then leads a reversal of the Josephson current

$$I \propto \frac{\partial E}{\partial \varphi} \propto \sin\varphi \to -I$$

Superconducting spintronics

The new physical phenomena combing spintronics and superconductivity lead to novel applications in quantum information processing

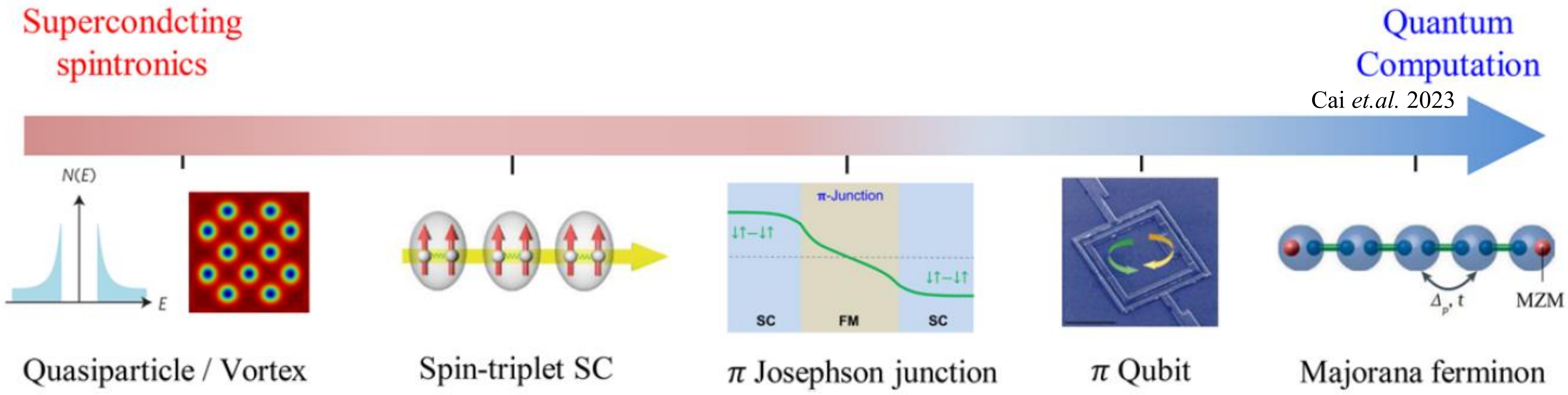

Enhancing spin lifetime

Large magnetoresistance

Giant thermoelectric effects

Control T_c through spin-injection

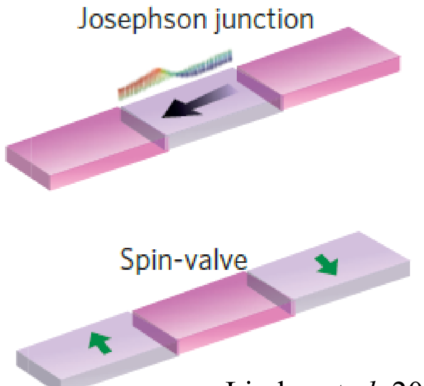

Linder *et.al.* 2015

Control 0 - π Josephson junction by ferromagnetic spin valve

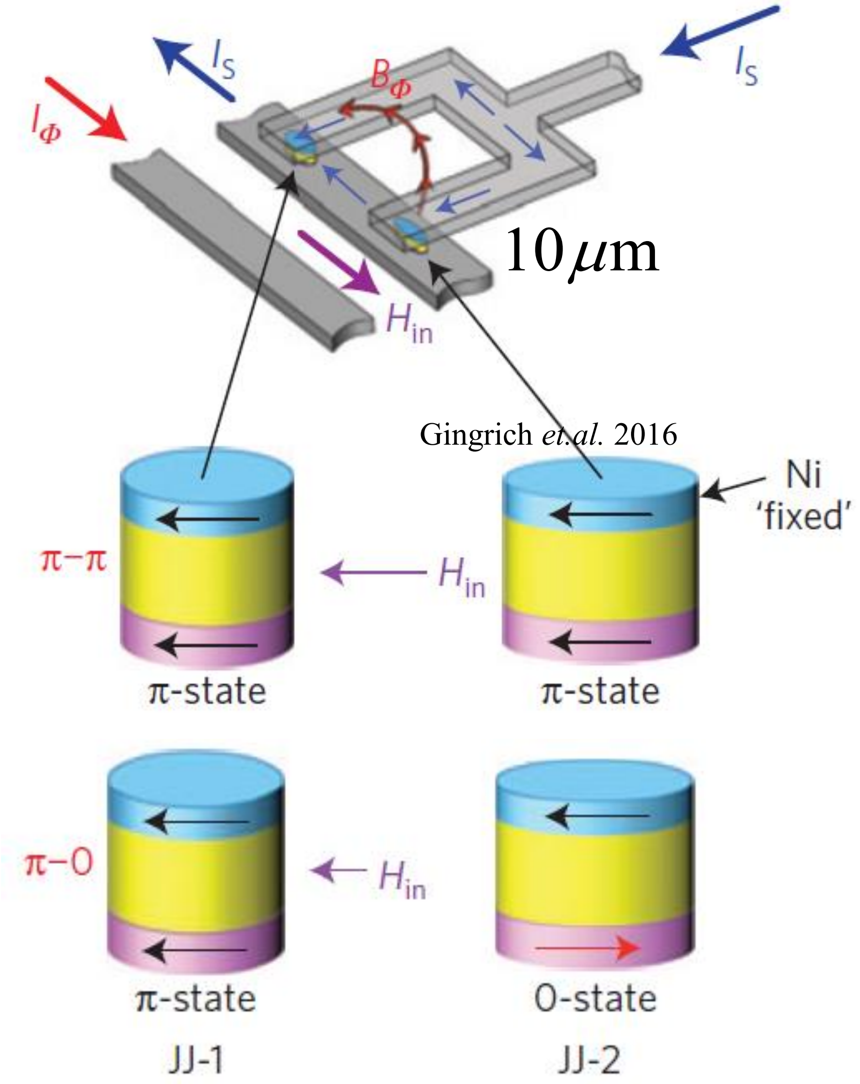

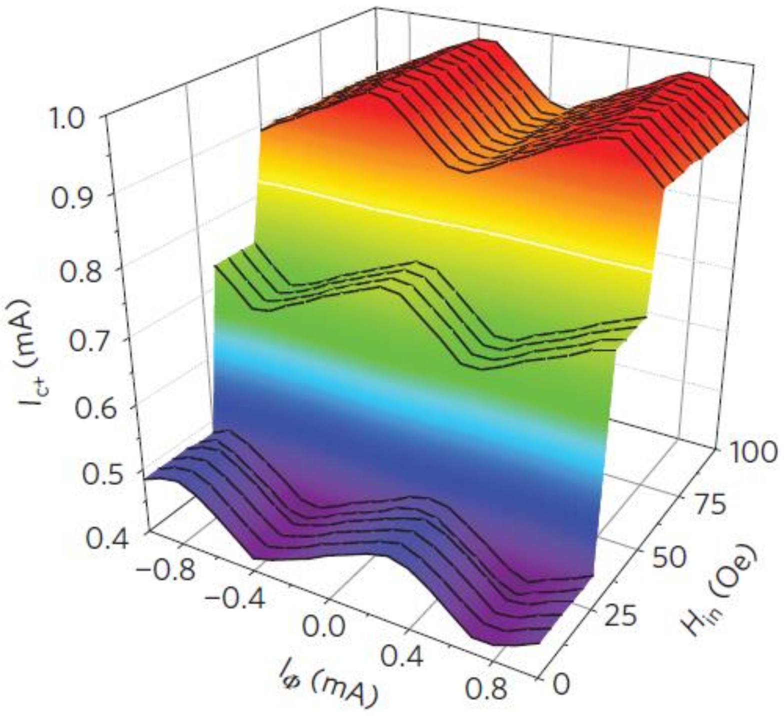

S/F$_1$/N/F$_2$/S junction: 0 - π transition induced by magnetization of ferromagnetic layers

Constructing superconducting qubit with ferromagnetic π Josephson junction

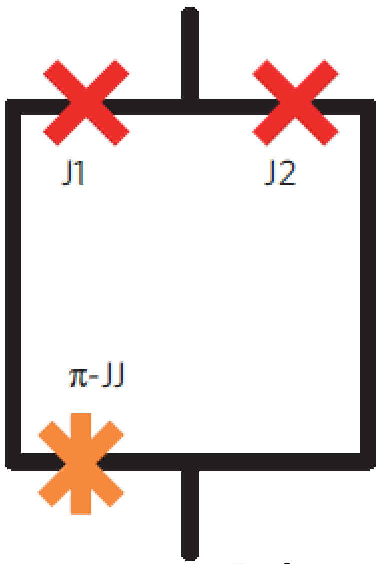

Feofanov *et.al.* 2010

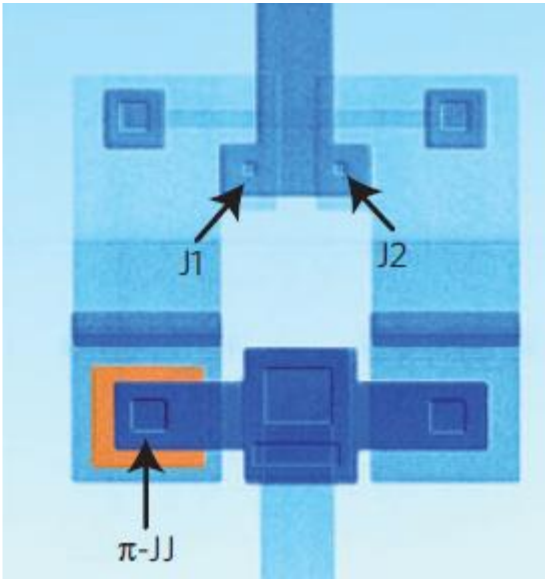

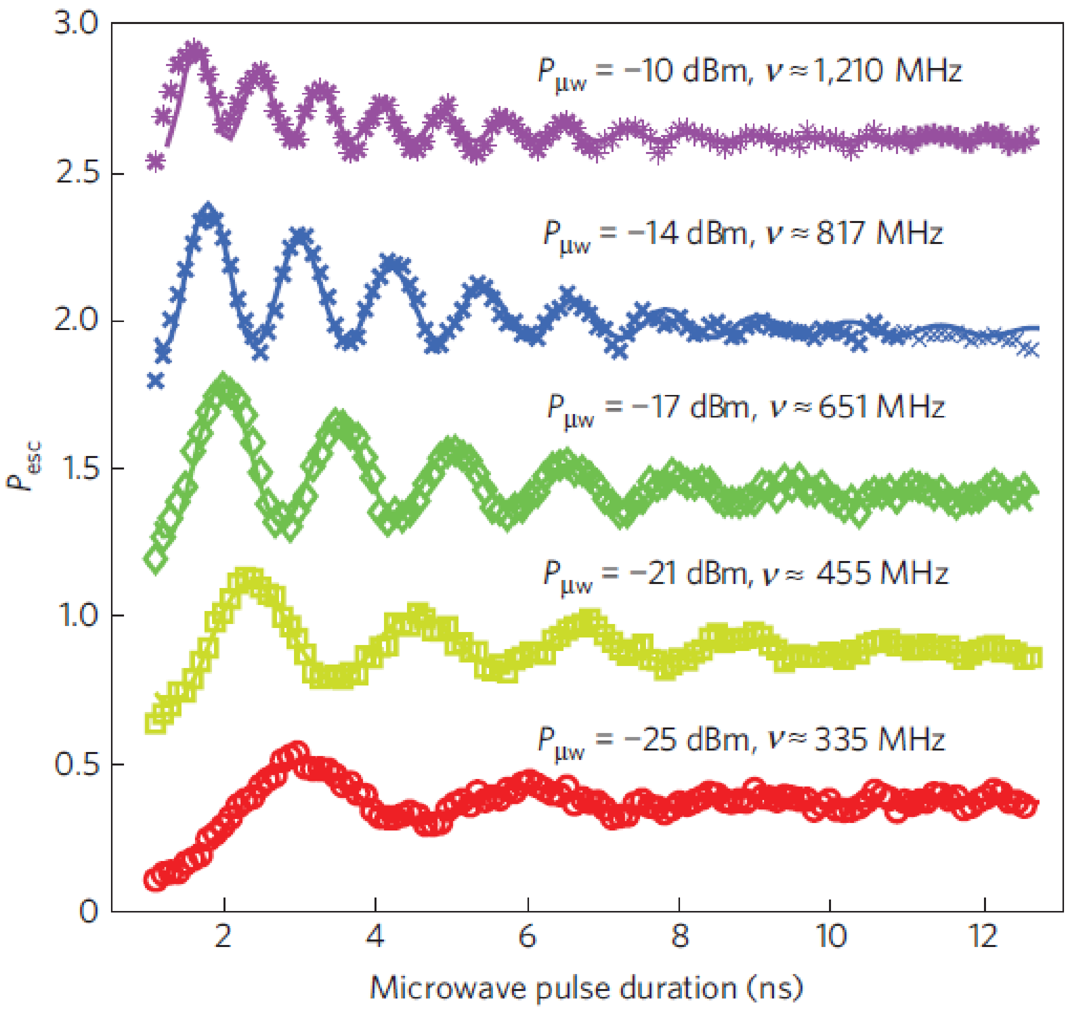

π junction as effective flux through the SQUID

Zero magnetic field leads to longer coherence time

Larger-scale integration by reducing qubit size

Beyond one-dimensional junctions

The short Josephson junction (1D junction)

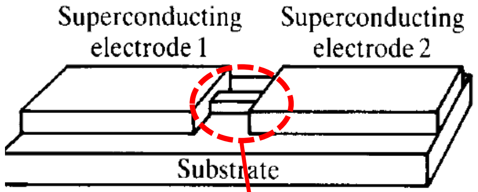

Tinkham 1996

1D transport channel

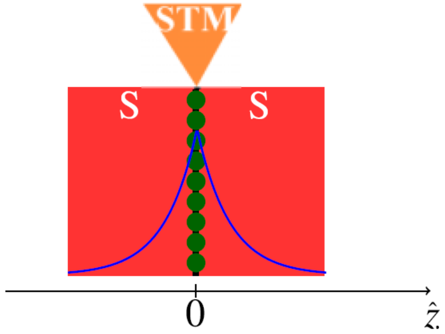

Costa *et.al.* 2018

The long Josephson junctions (LJJ) refers to junctions where the size of the barrier exceed given characteristic length in some directions (2D junction)

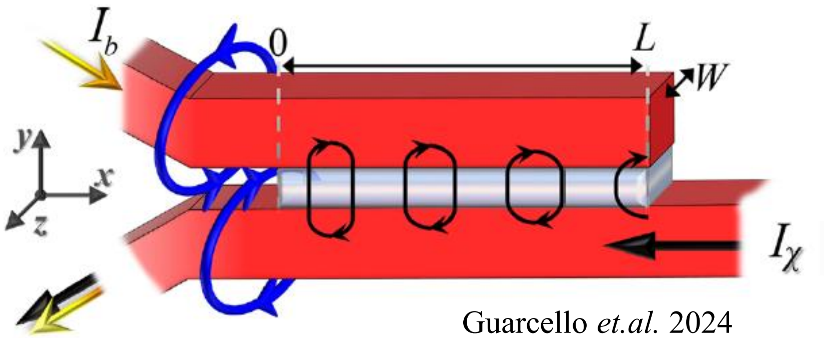

Guarcello *et.al.* 2024

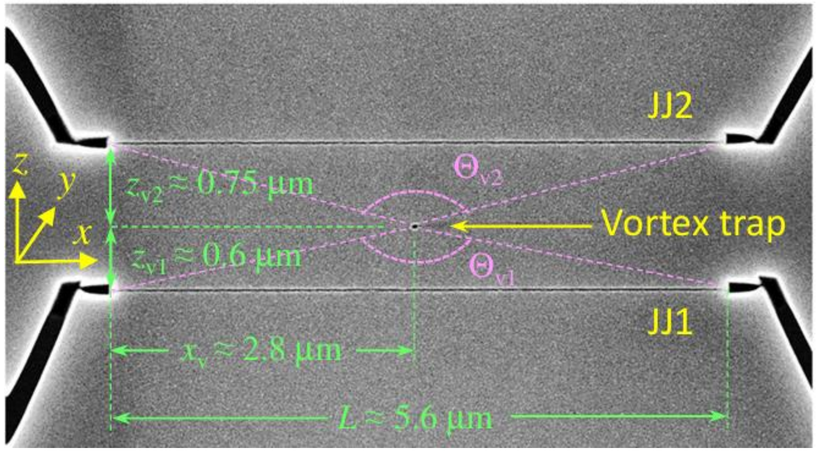

Golod *et.al.* 2022

Example of interface beyond 1D: Majorana bound states

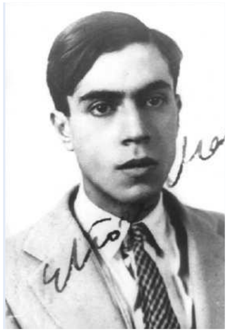

$$\hat{\gamma} = \hat{\gamma}^{\dagger}$$

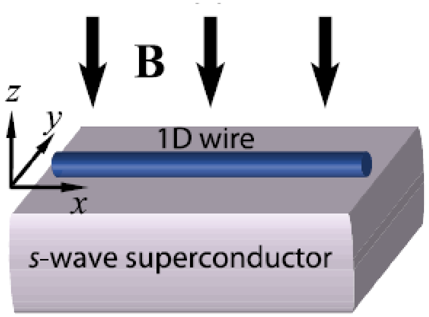

Alicea *et.al.* 2012

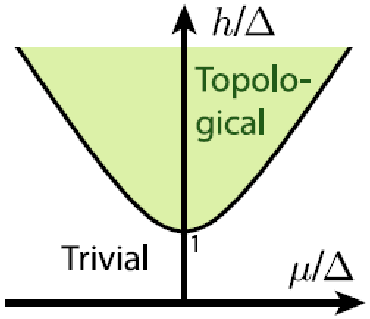

Topological

superconductor

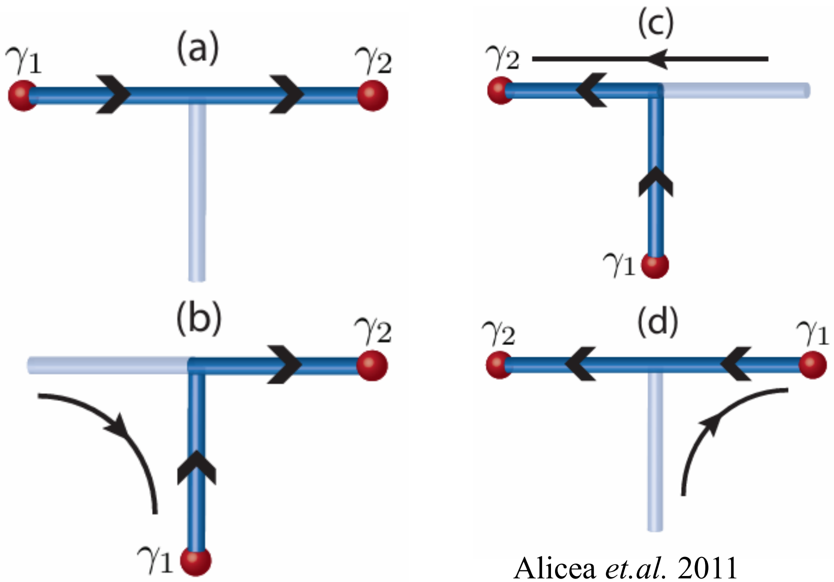

Alicea *et.al.* 2011

$$\hat{\gamma}_i \rightarrow \sum_j s_{ij}\hat{\gamma}_j$$

$$\hat{\gamma}_j \rightarrow \sum_i s_{ji}\hat{\gamma}_i$$

In recent years, the research on planar Josephson junctions has been gaining increasing attention

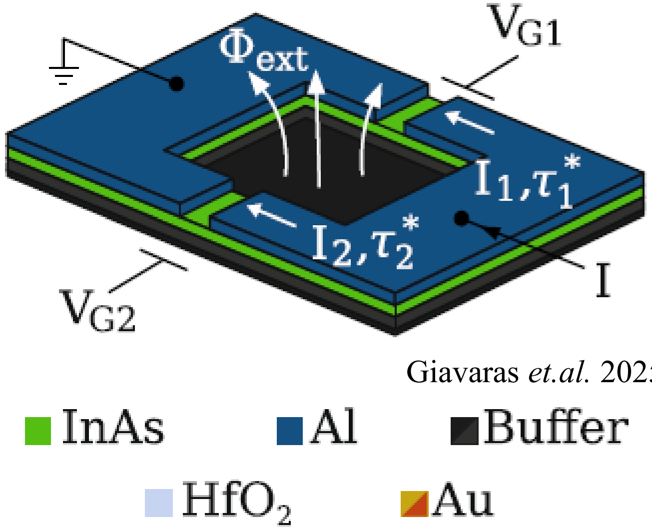

Giavaras *et.al.* 2025

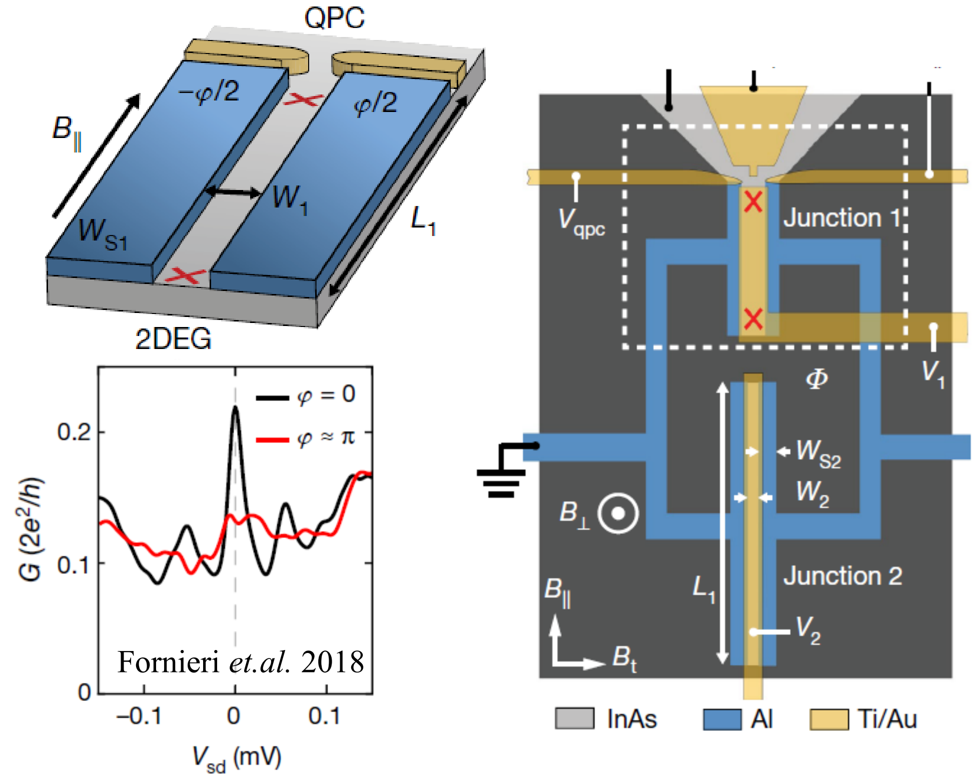

Fornieri *et.al.* 2018

Junction area: $8.12\mu\text{m} \times 8.12\mu\text{m} = 65.93\mu\text{m}$

Typical magnetic field: $B = \dfrac{0.5\Phi_0}{S} = 0.031\text{mT}$

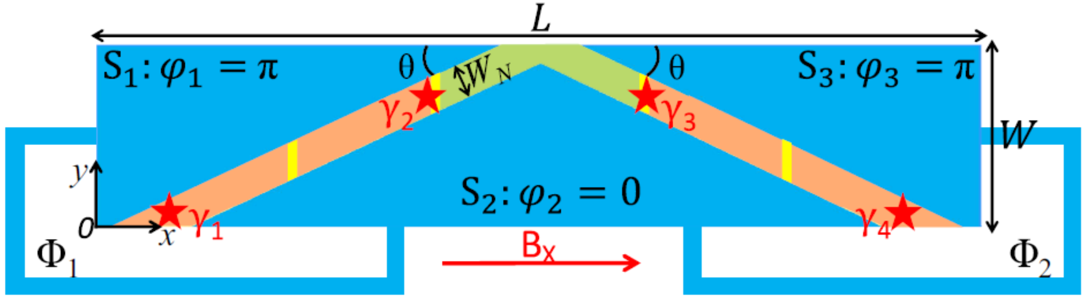

Zhou *et.al.* 2022; 2024

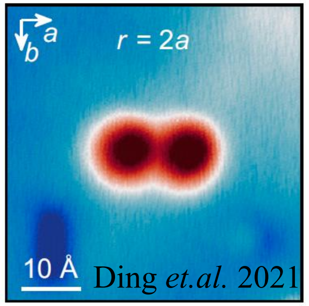

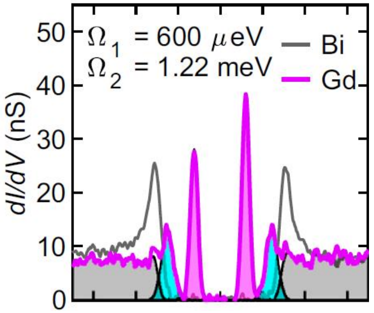

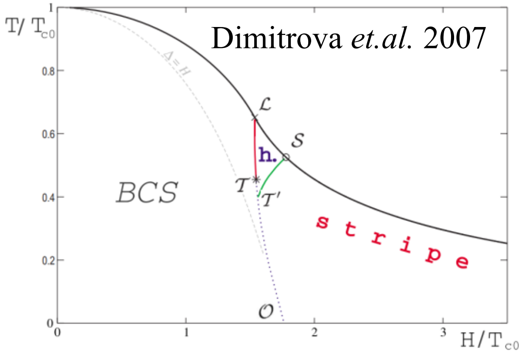

YSR bound state

helical phase

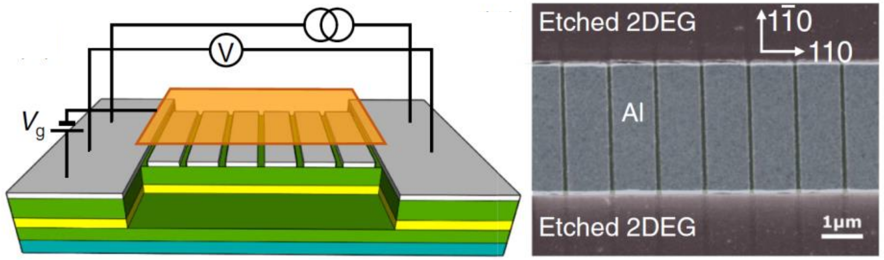

$\hat{c}^{\dagger}_{k\uparrow}\hat{c}^{\dagger}_{-k\downarrow}$

superconductor

$\hat{\mathbf{S}}_i \cdot \hat{\mathbf{S}}_j$

ferromagnet

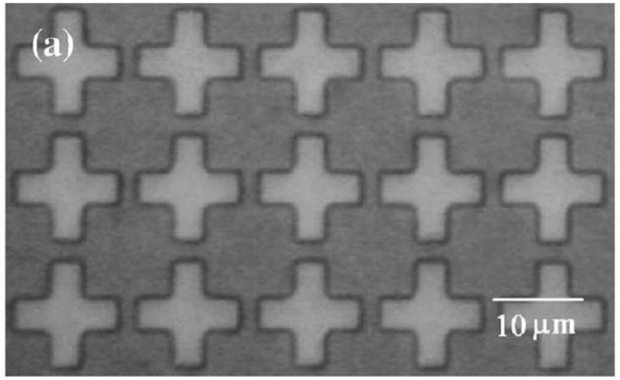

Baek et.al. 2005

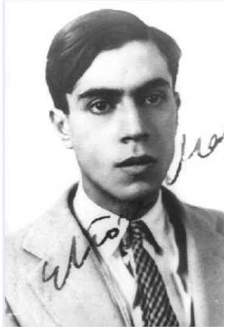

$\hat{\gamma} = \hat{\gamma}^{\dagger}$

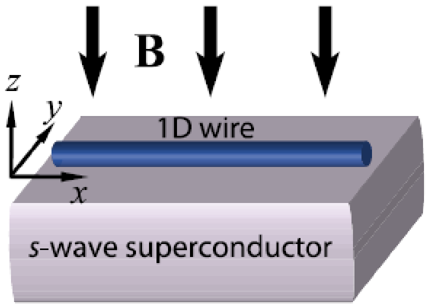

Alicea et.al. 2012

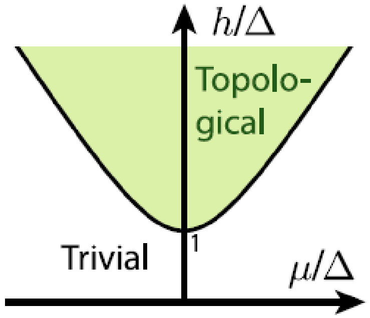

Topological superconductor

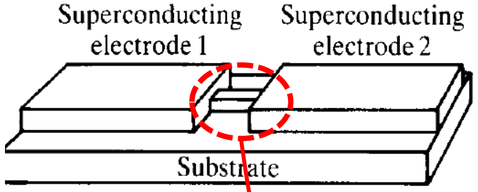

Tinkham 1996

1D channel

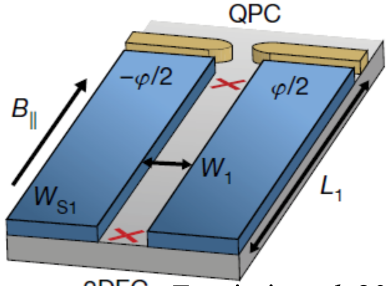

Fornieri et.al. 2018

We aim to investigate whether the introduction of **transverse subgap modes** can lead to new physical effects in the competition between superconducting and ferromagnetic orders

Outline

I. Introduction

1. Superconductivity and the Josephson effect
2. Applications of the Josephson junctions

II. Two-dimensional magnetic Josephson junctions

1. Interplay of superconductivity and magnetic orders
2. Superconducting spintronics
3. Beyond one-dimensional junctions

III. Transverse subgap modes

1. The model
2. Flat-dispersion
3. Domain walls and applications

IV. $0-\pi$ transitions in two-dimensional junctions

1. The Josephson current
2. Implications in experiments

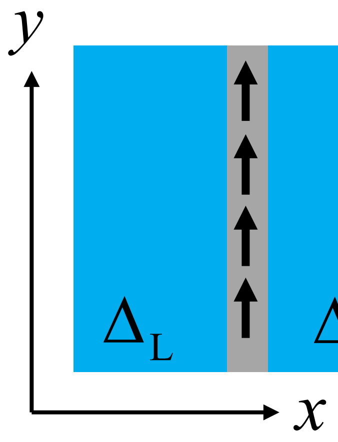

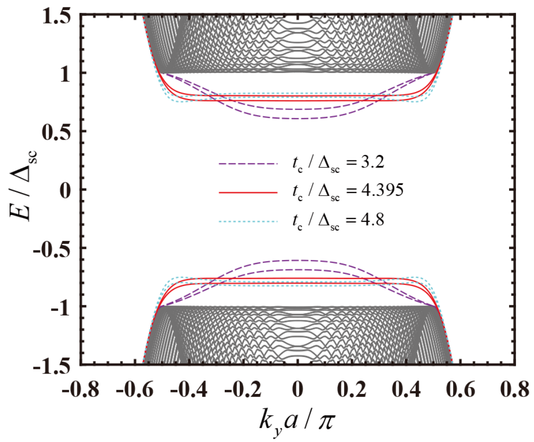

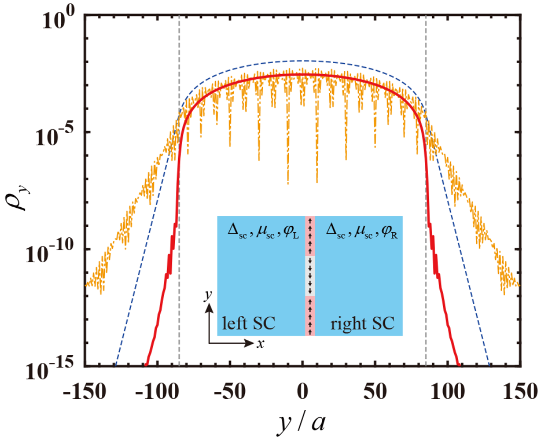

The model

We investigate a superconductor/ferromagnet/superconductor junction with large lateral size

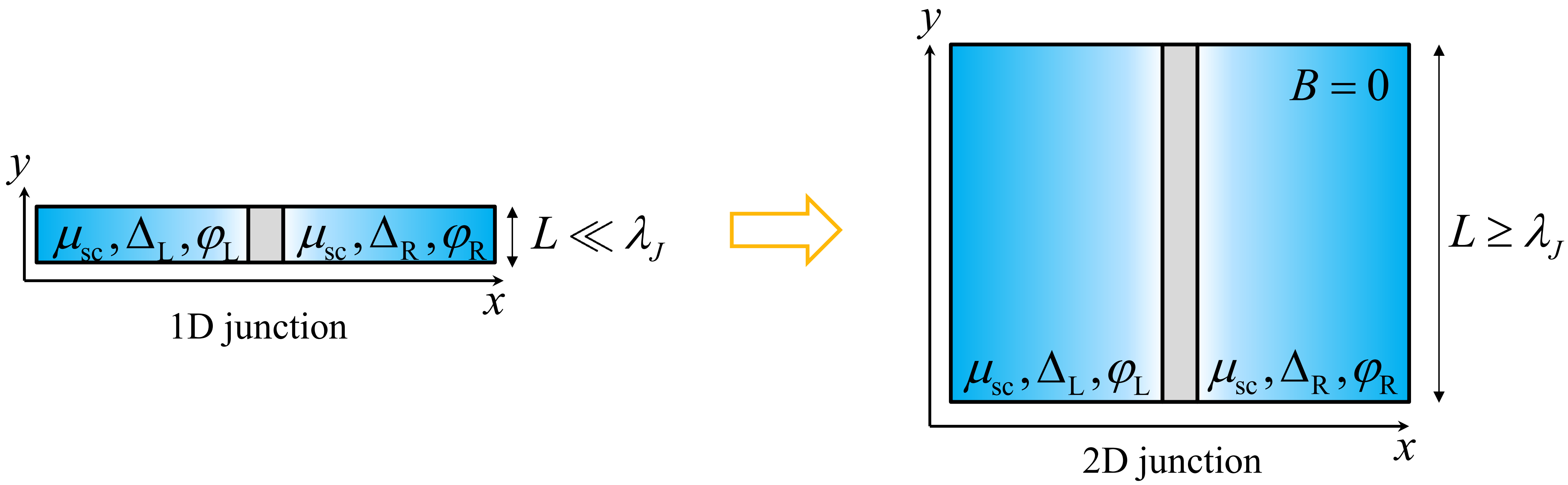

Josephson penetration depth $\lambda_J = \sqrt{\dfrac{\Phi_0}{2\pi \mathcal{L} J_c W}}$ (typical on the order of 0.1mm)

Guarcello *et.al.* 2024; Fossheim 2021

Subgap modes in 1D junction:

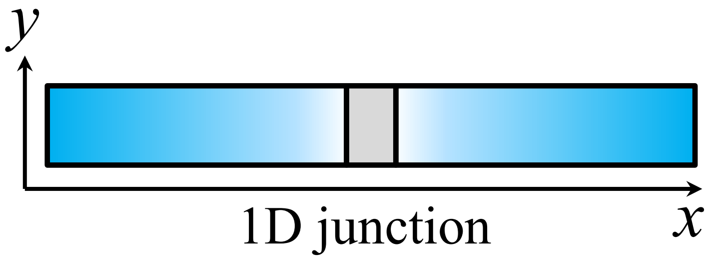

Model Hamiltonian

$$\hat{H} = \frac{1}{2}\int dx \hat{\Psi}(x)^\dagger \mathcal{H}_{\mathrm{BdG}}(x)\hat{\Psi}(x)$$

$$\mathcal{H}_{\mathrm{BdG}}(x) = \left[\left(-\frac{\hbar^2}{2m}\frac{\partial^2}{\partial x^2} - \mu_{\mathrm{sc}}\right)\hat{\tau}^z + \left(\Delta(x)\hat{\tau}^+ + \mathrm{h.c.}\right)\right]\hat{\sigma}^0 + k_{\mathrm{sc}}^{-1}\delta(x)\left(\lambda_{\mathrm{sc}}\hat{\sigma}^0 + \lambda_{\mathrm{M}}\hat{\sigma}^z\right)\hat{\tau}^z$$

Solve the BdG equation together with the matching conditions

$$\mathcal{H}_{\mathrm{BdG}}(x)\Psi(x) = E_n^{\pm}\Psi(x)$$

$$\Psi(x)\big|_{x=0^-} = \Psi(x)\big|_{x=0^+} \qquad \lim_{\delta x\to 0^+}\int_{-\delta x}^{\delta x} dx \mathcal{H}_{\mathrm{BdG}}(x)\Psi(x) = 0$$

Spin-degeneracy was lifted and in general, two subgap modes are observable

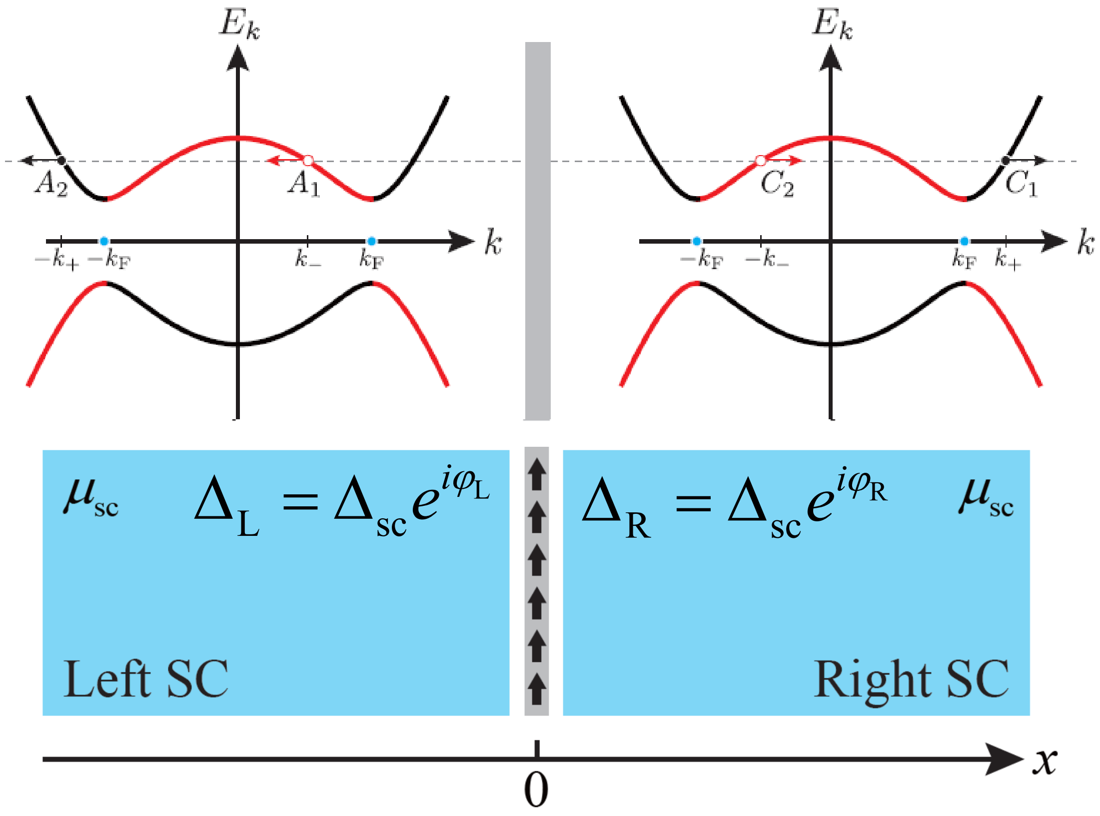

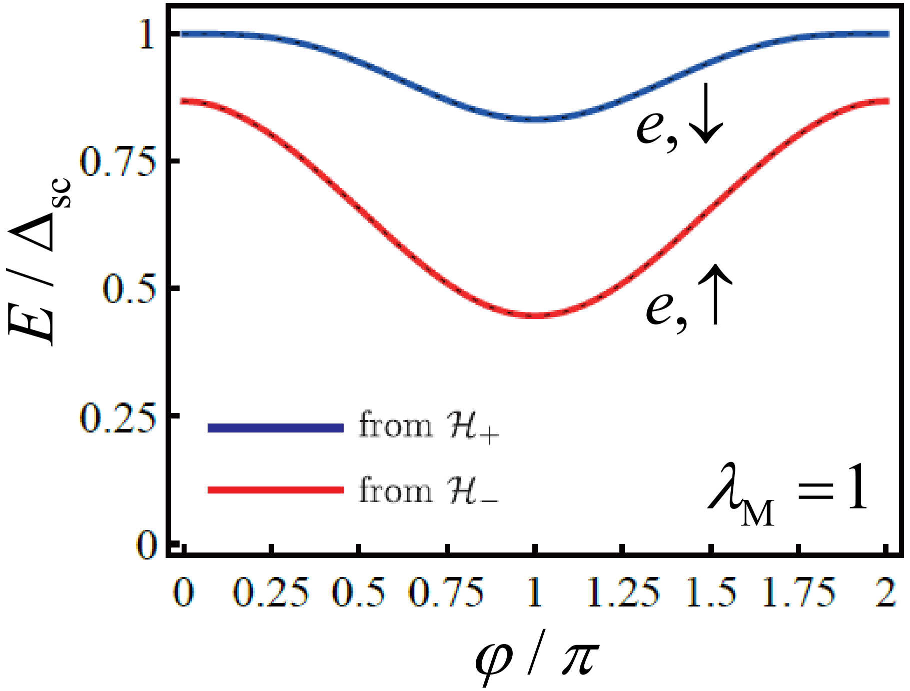

Superconducting phase difference $\varphi = \varphi_L - \varphi_R$

Subgap modes in 2D junction:

Model Hamiltonian (tight-binding)

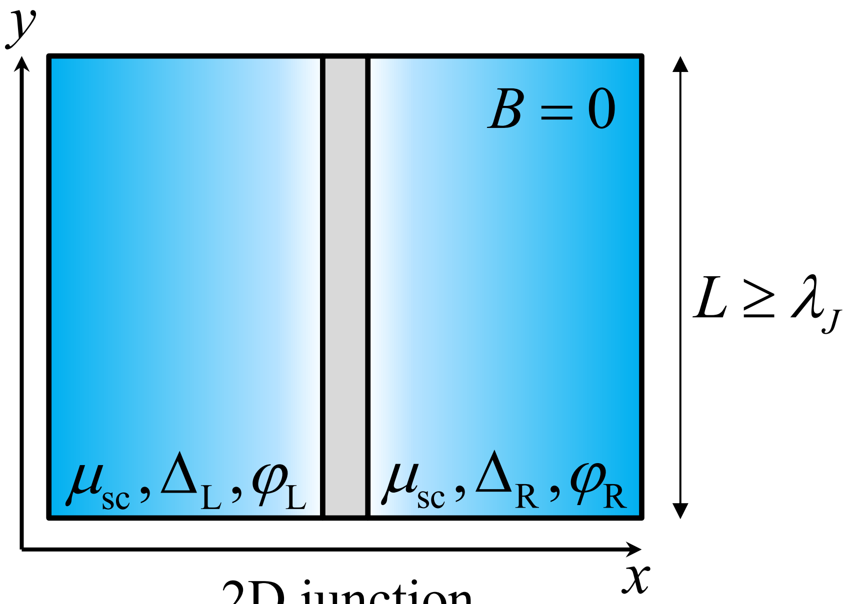

2D junction

$$\hat{H} = \hat{H}_{\mathrm{L}} + \hat{H}_{\mathrm{R}} + \hat{H}_{\mathrm{fm}} + \hat{H}_{\mathrm{tun}}$$

$$\hat{H}_{\mathrm{L/R}} = -\frac{t_{\mathrm{sc}}}{2} \sum_{x=1}^{N_x} \sum_{y=1}^{N_y} \sum_{\sigma} \left(\hat{c}^{\dagger}_{\mp x,y,\sigma} \hat{c}_{\mp x,y+1,\sigma} + \hat{c}^{\dagger}_{\mp x,y,\sigma} \hat{c}_{\mp x+1,y,\sigma} + \mathrm{h.c.} \right)$$

$$+\Delta_{\mathrm{L/R}} \sum_{x,y} \left(\hat{c}^{\dagger}_{\mp x,y,\uparrow} \hat{c}^{\dagger}_{\mp x,y,\downarrow} + \mathrm{h.c.} \right) - \mu_{\mathrm{sc}} \sum_{x,y,\sigma} \hat{c}^{\dagger}_{\mp x,y,\sigma} \hat{c}_{\mp x,y,\sigma}$$

$$\hat{H}_{\mathrm{fm}} = \sum_{y} \left[\lambda_{\mathrm{M}} \left(\hat{f}^{\dagger}_{y,\uparrow} \hat{f}_{y,\uparrow} - \hat{f}^{\dagger}_{y,\downarrow} \hat{f}_{y,\downarrow} \right) - \mu_{\mathrm{fm}} \sum_{\sigma} \hat{f}^{\dagger}_{y,\sigma} \hat{f}_{y,\sigma} \right] - \frac{t_{\mathrm{fm}}}{2} \sum_{\sigma} \left(\hat{f}^{\dagger}_{y,\sigma} \hat{f}_{y+1,\sigma} + \mathrm{h.c.} \right)$$

$$\hat{H}_{\mathrm{tun}} = -\frac{t_{\mathrm{c}}}{2} \sum_{x=\pm 1} \sum_{y} \sum_{\sigma} \left(\hat{c}^{\dagger}_{x,y,\sigma} \hat{f}_{y,\sigma} + \mathrm{h.c.} \right)$$

$$\Delta_{\mathrm{L/R}} = \Delta_{\mathrm{sc}} \exp\left[i\varphi_{\mathrm{L/R}} \right]$$

Extending to the 2D junction case, with periodic boundary long the lateral (y) direction

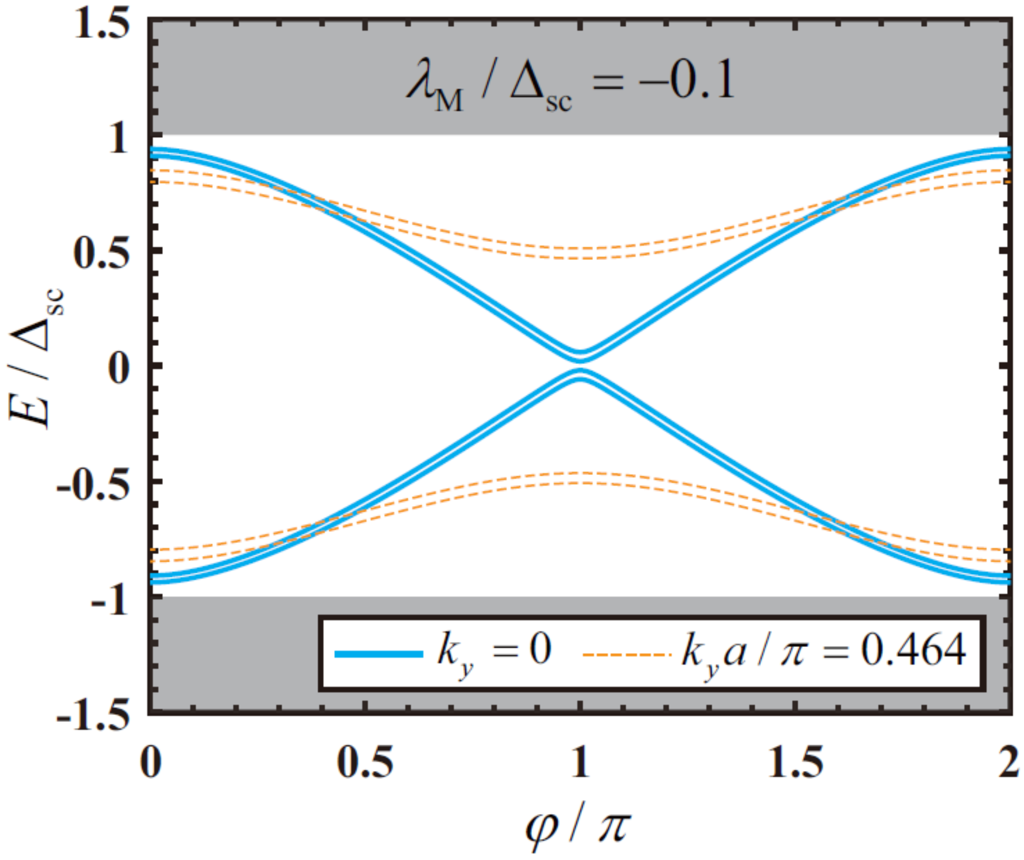

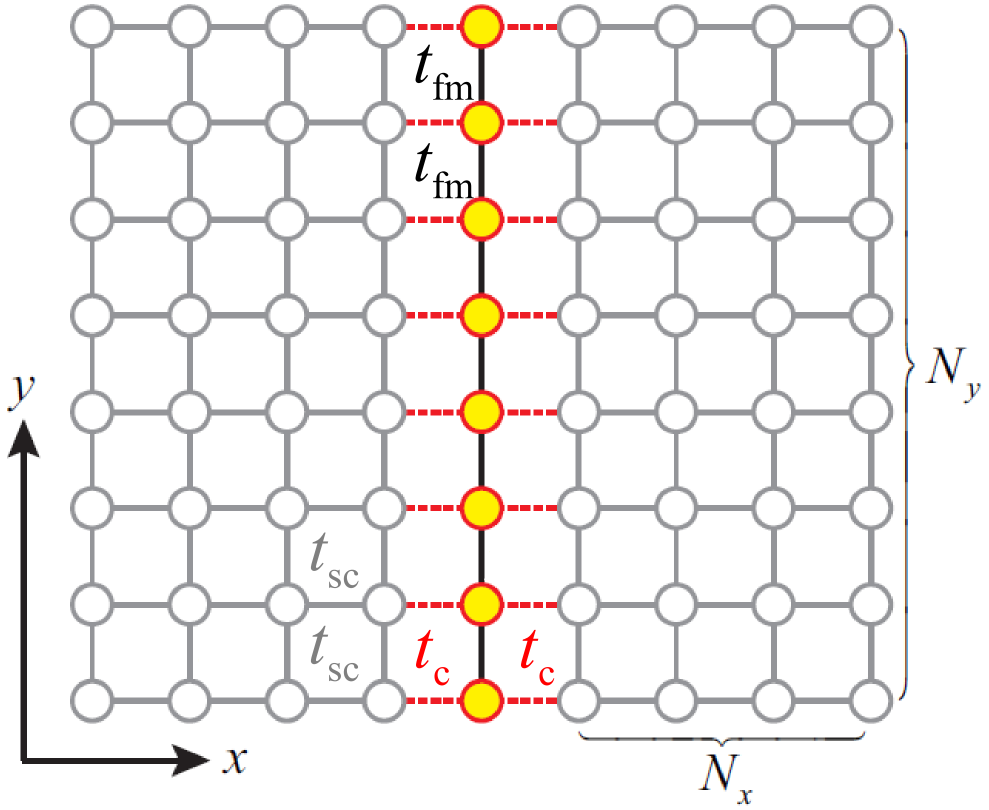

Translational invariance long y $\quad -\frac{\hbar^2\nabla^2}{2m} - \mu_{sc} \quad \Rightarrow \quad \mu_{sc} \to \mu_{sc}(k_y) = \mu_{sc} - \frac{\hbar^2 k_y^2}{2m}$

Flat-dispersion

Energy spectrum as a function of k_y at fixed φ shown the competition between the proximity effect and the spin splitting

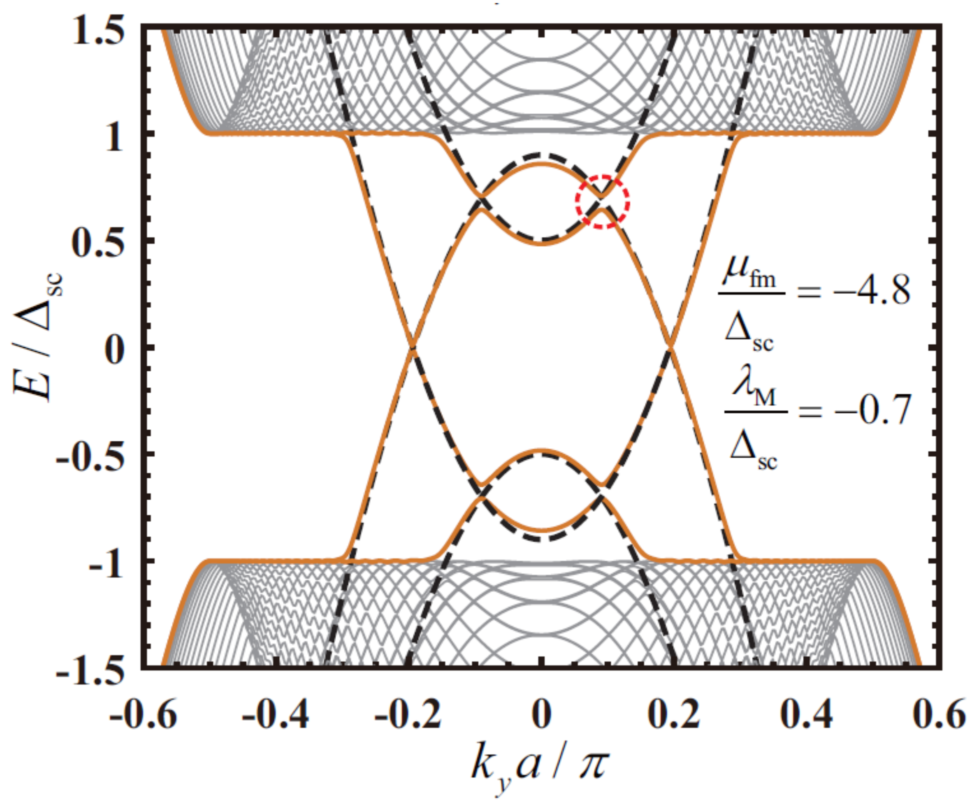

Weak tunneling regime $t_c < \Delta_{sc}$

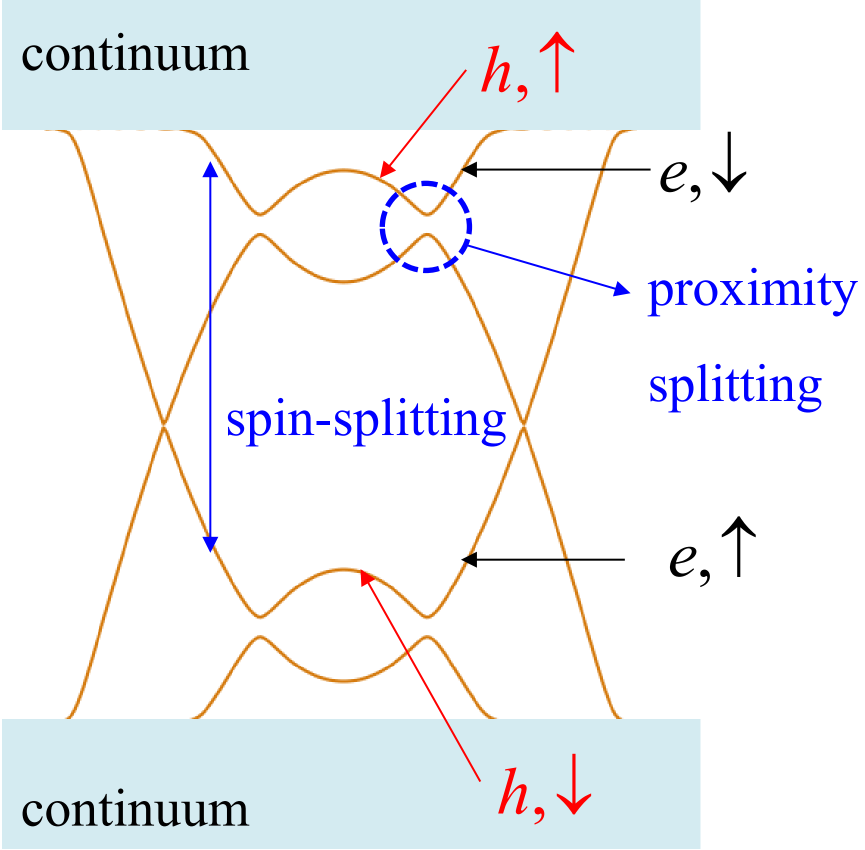

The proximity induced splitting gap agrees well to the effective Hamiltonian obtained by integrating out the degree of freedom of the superconductors

$$\hat{H}_{\mathrm{eff}} = \hat{H}_{\mathrm{fm}} + \left(\Delta_{\mathrm{eff}} \sum_{y} \hat{f}^{\dagger}_{y,\uparrow} \hat{f}^{\dagger}_{y,\downarrow} + \mathrm{h.c.} \right)$$

$$\Delta_{\mathrm{eff}} = \frac{t_{\mathrm{c}}^{2}}{4} \left(\frac{1}{\Delta_{\mathrm{L}}^{*}} + \frac{1}{\Delta_{\mathrm{R}}^{*}} \right)$$

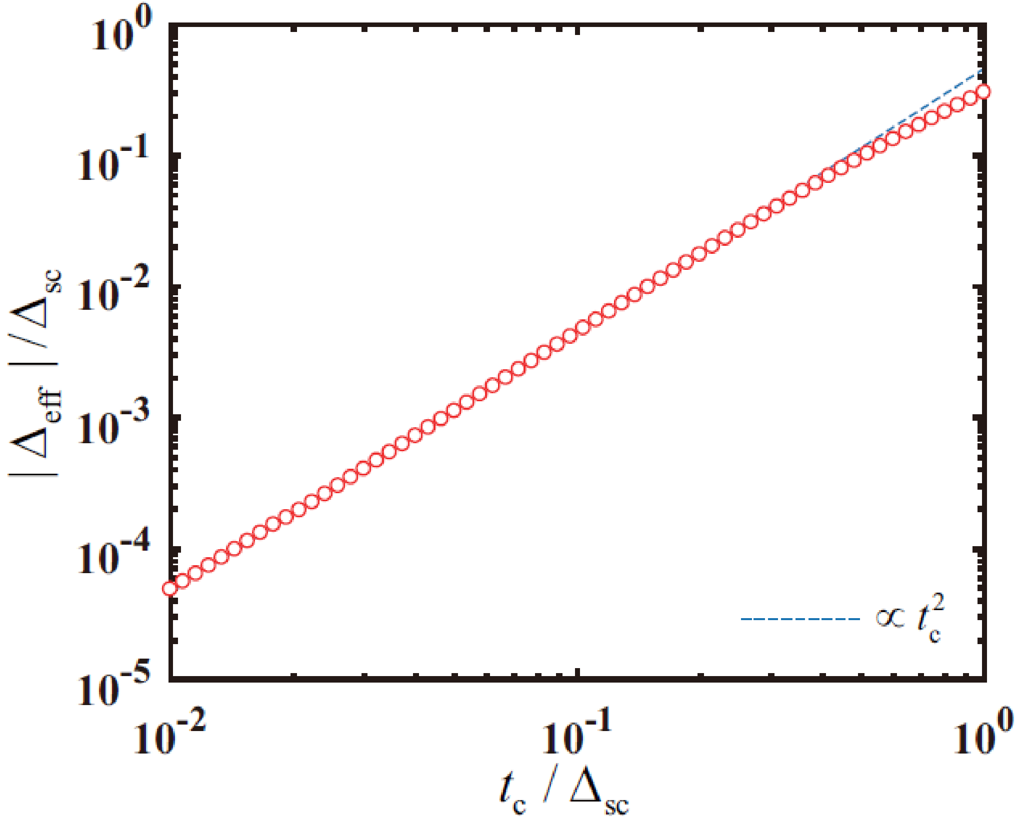

t_{c}: the tunneling coupling between superconductor and ferromagnetic barrier

Stronger proximity induced gap leads to nearly flat-dispersion of the subgap mode

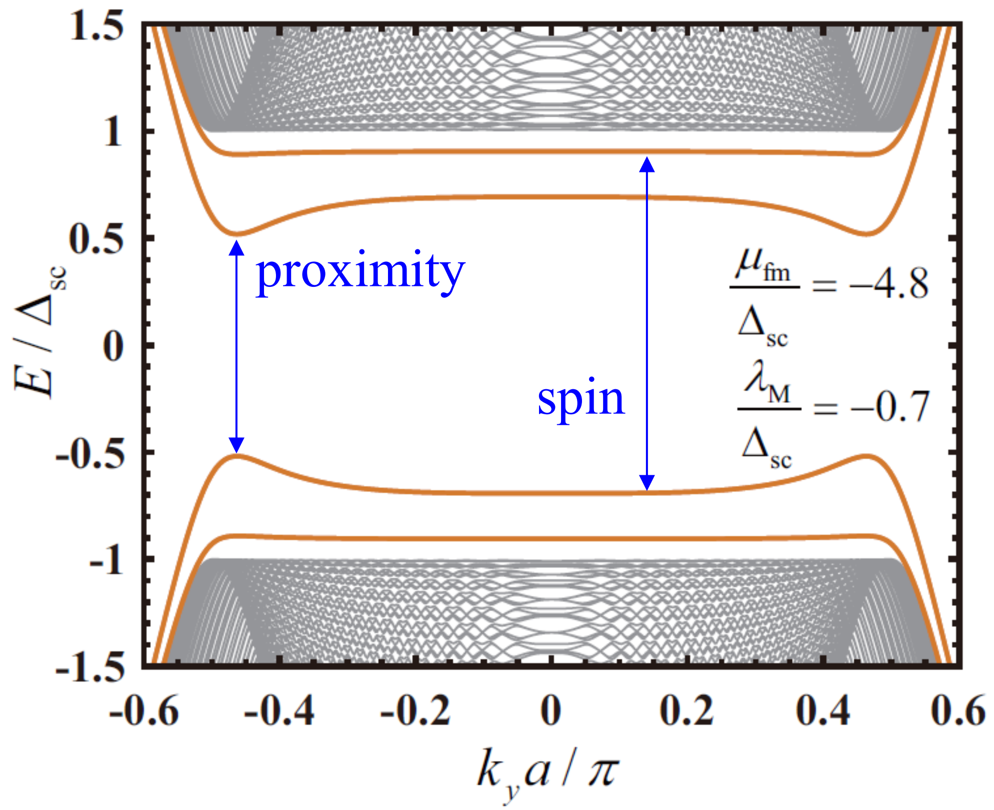

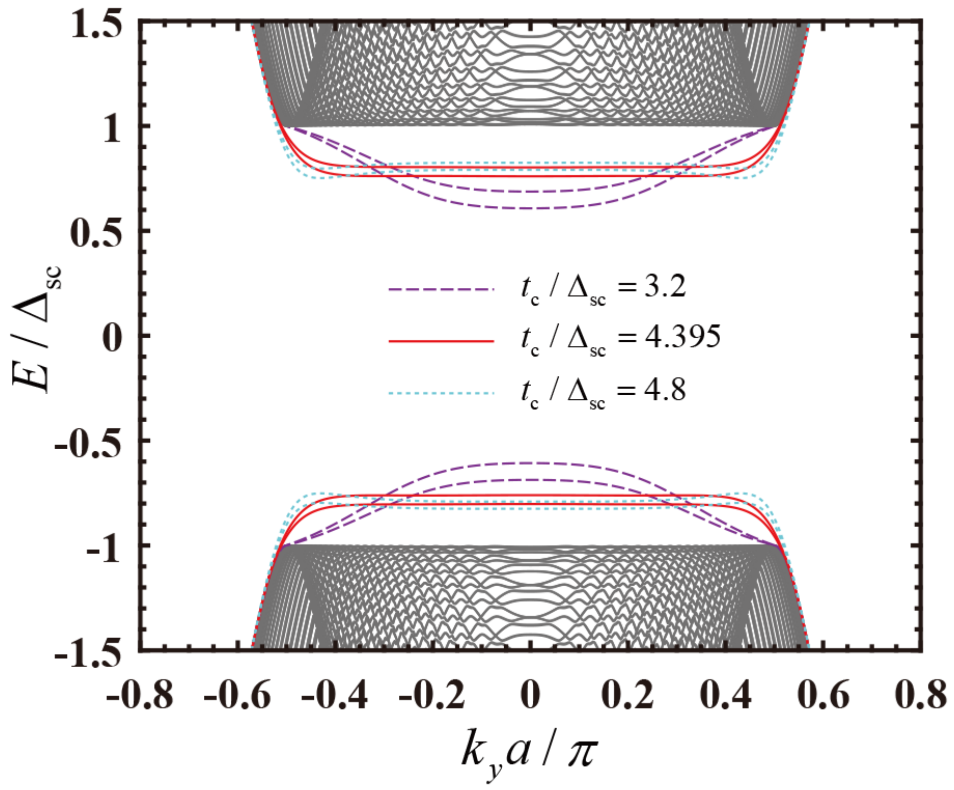

Strong tunneling regime $t_c \gg \Delta_{sc}$

Particular t_c / Δ_{sc} ratio enables the realization of nearly flat subgap modes

Domain walls and applications

The flat-dispersion of subgap modes modifies the wave function of quasi-particles confined between domain walls

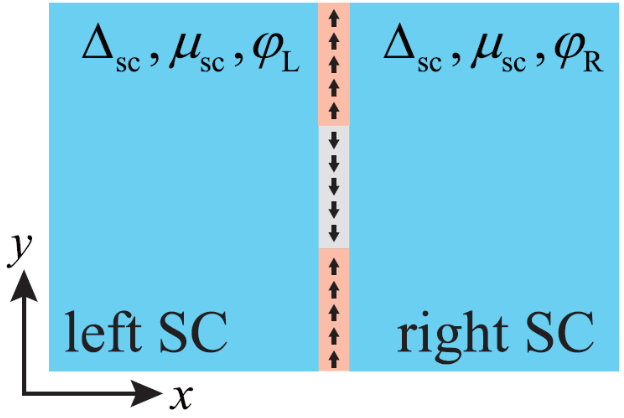

Flat-dispersion

$$\frac{\hbar^2 k_y^2}{2m}$$

$\Rightarrow$

Large effective mass

$$m_{\text{eff}}$$

The influence of the flat-dispersion revealed in the real-space distribution of the quasi-particle

$$\sum_i \sum_{y\in \mathrm{D}_i} \lambda_{\mathrm{M},i}\left(\hat{f}^\dagger_{y,\uparrow}\hat{f}_{y,\uparrow} - \hat{f}^\dagger_{y,\downarrow}\hat{f}_{y,\downarrow}\right)$$

$$\hat{\gamma}_\varepsilon = \sum_{y,\sigma}\left(u_{y,\sigma}\hat{f}_{y,\sigma} + v_{y,\sigma}\hat{f}^\dagger_{y,\sigma}\right) + \hat{\gamma}_{\mathrm{sc}}$$

$$\rho_y = \sum_\sigma \left(|u_{y,\sigma}|^2 + |v_{y,\sigma}|^2\right)$$

Distribution of quasi-particle along the junction

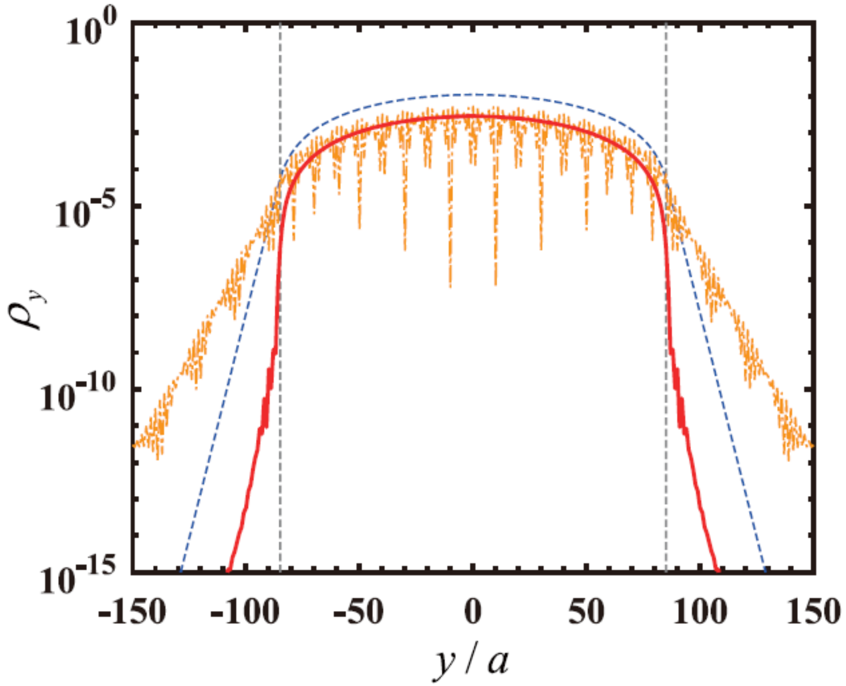

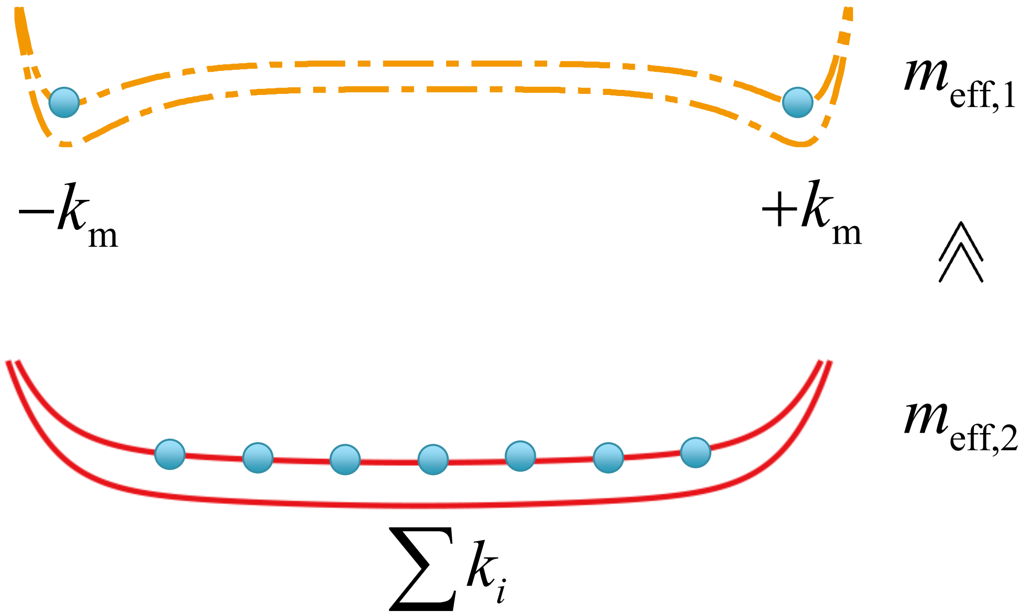

Change the relative spin-splitting of neighboring domain walls enable switching of the quasi-particle

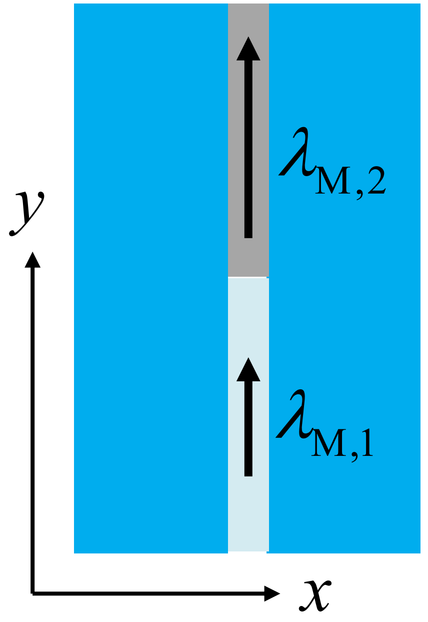

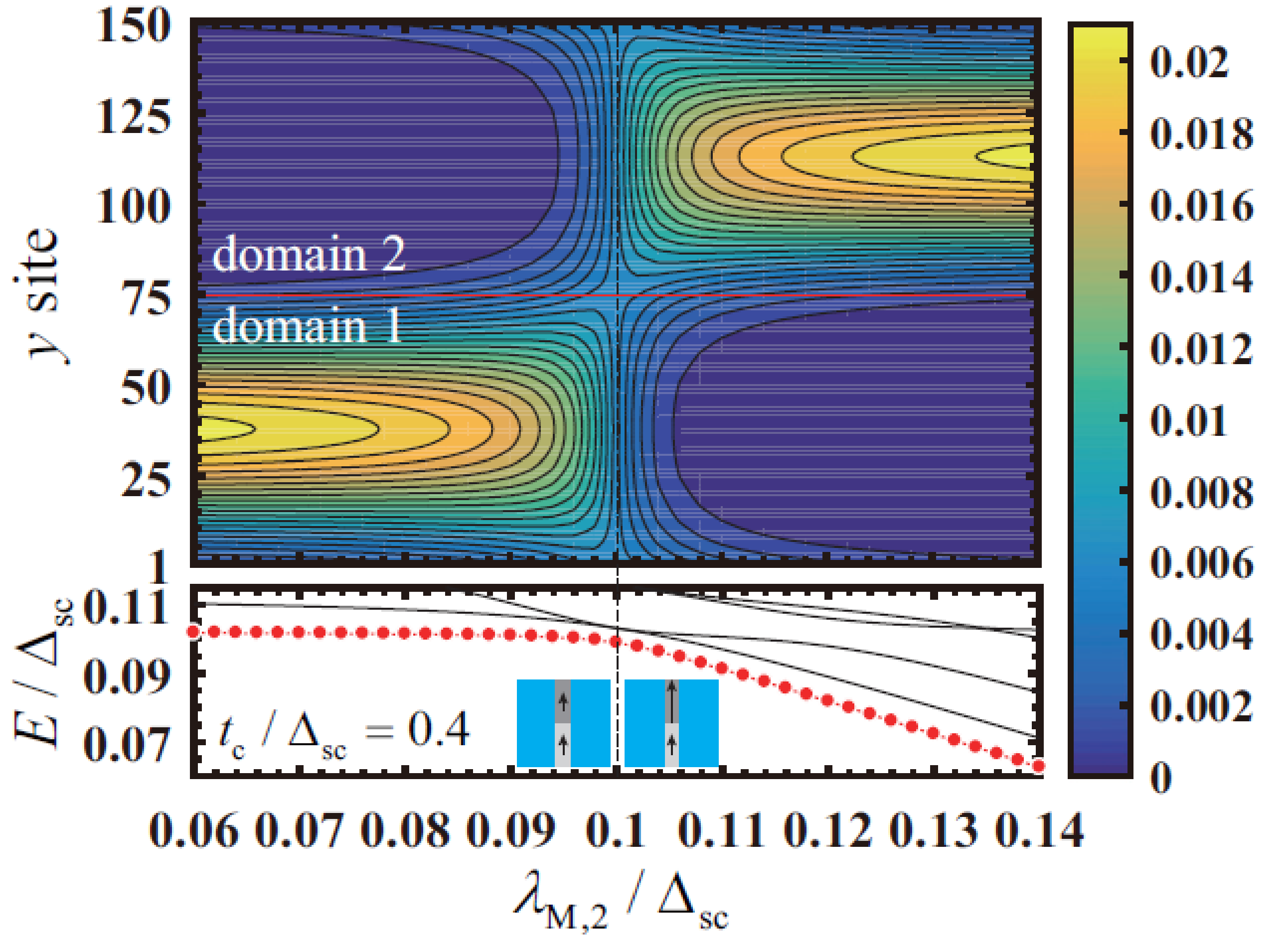

Outline

I. Introduction

1. Superconductivity and the Josephson effect
2. Applications of the Josephson junctions

II. Two-dimensional magnetic Josephson junctions

1. Interplay of superconductivity and magnetic orders
2. Superconducting spintronics
3. Beyond one-dimensional junctions

III. Transverse subgap modes

1. The model
2. Flat-dispersion
3. Domain walls and applications

IV. 0 - π transitions in two-dimensional junctions

1. The Josephson current
2. Implications in experiments

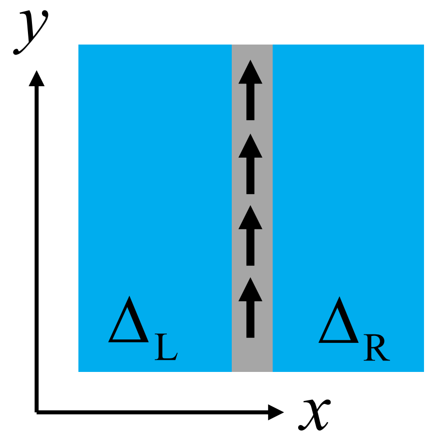

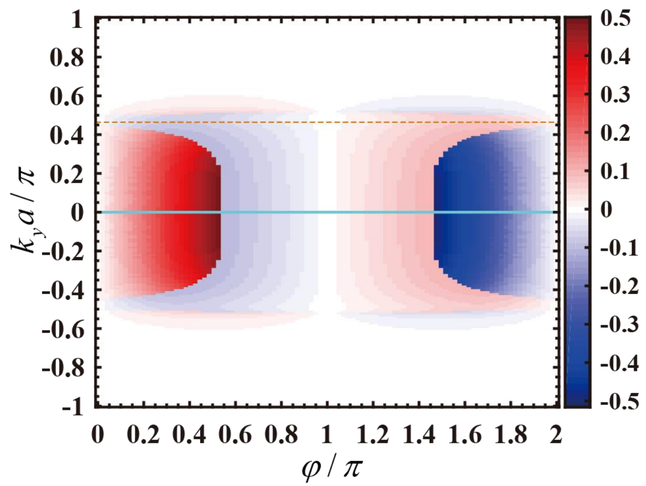

The Josephson current

The translational invariance along the lateral direction allows one to decompose the Josephson current into k_y dependent contributions

$$I_{\text{tot}}(\varphi)=\frac{2e}{\hbar}\int_{-k_*}^{k_*}dk_y\sum_{E_n\le 0}\left[\frac{\partial E_n(k_y)}{\partial\varphi}\tanh\frac{E_n(k_y)}{2k_BT}\right]=\int dk_y I_{k_y}(\varphi) \qquad k_*a=\cos^{-1}\left(-\frac{\mu_{\text{sc}}}{t_{\text{c}}}-1\right)$$

The current – phase relation is strongly modified by the transverse motion of the quasi – particles

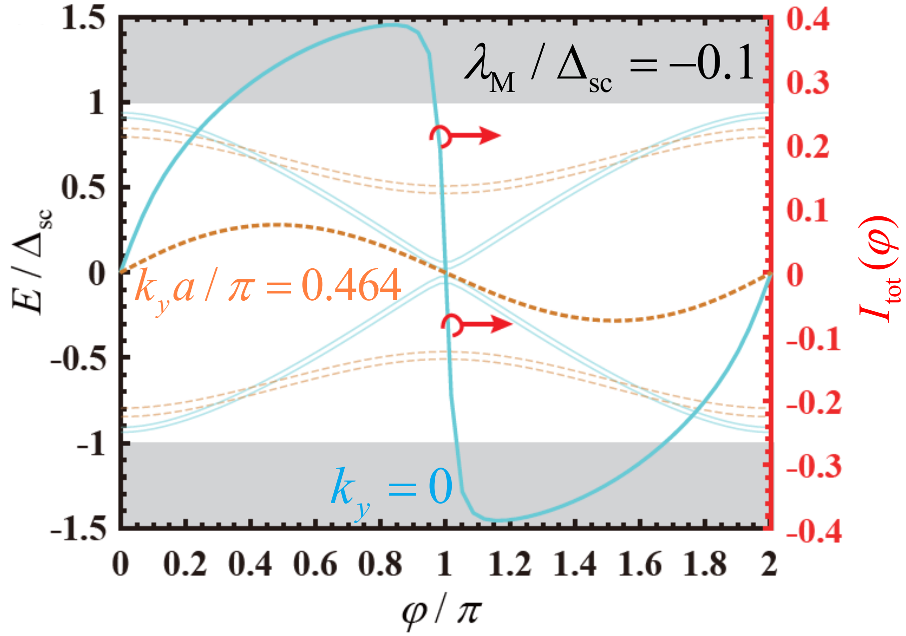

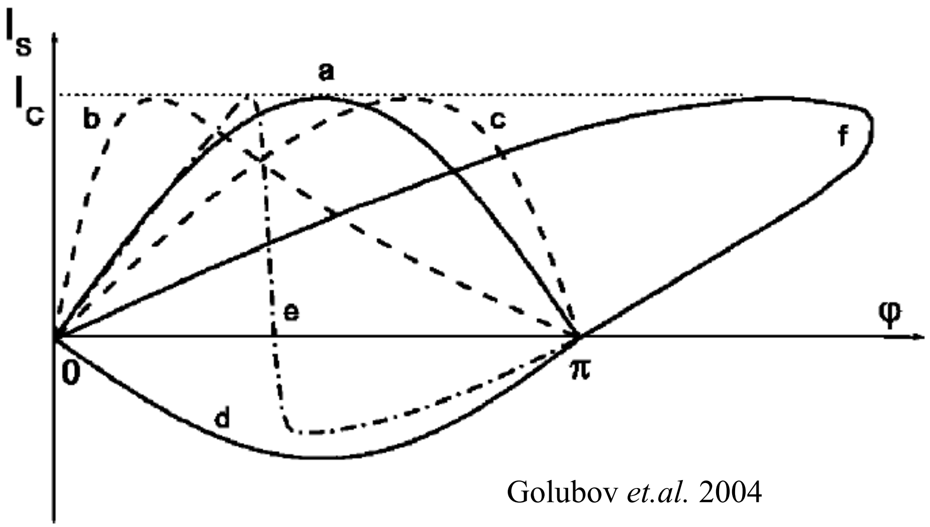

Golubov *et.al.* 2004

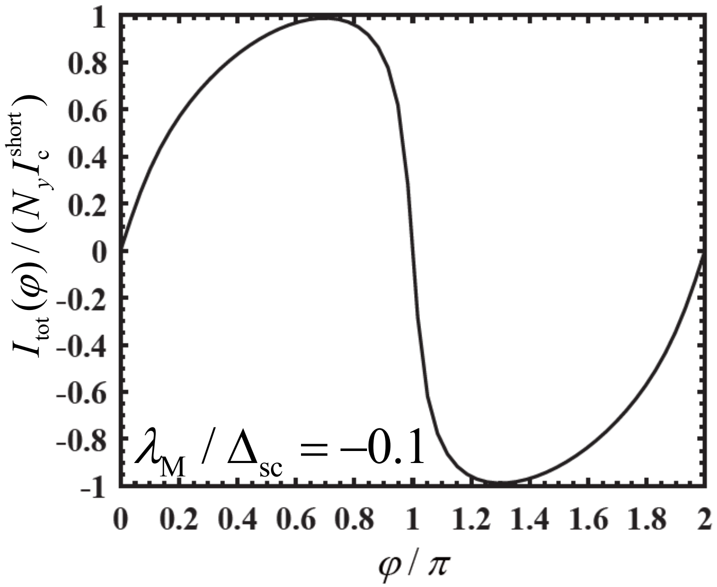

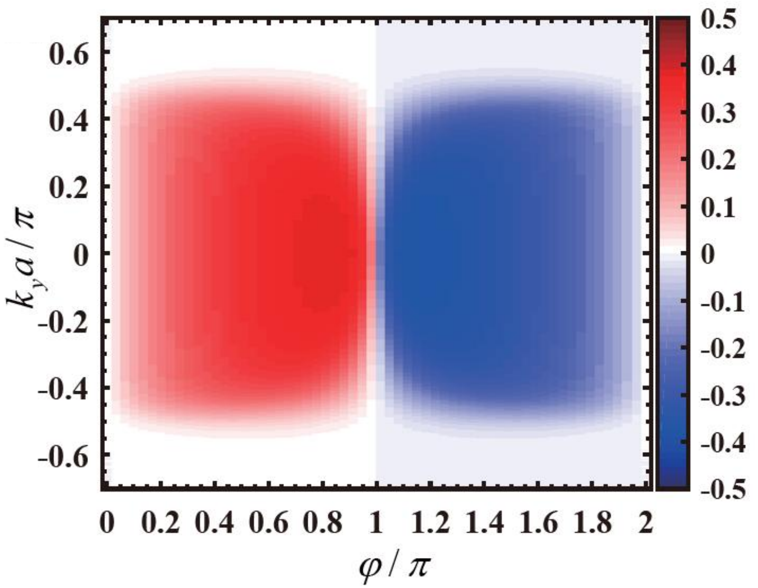

0 - junction

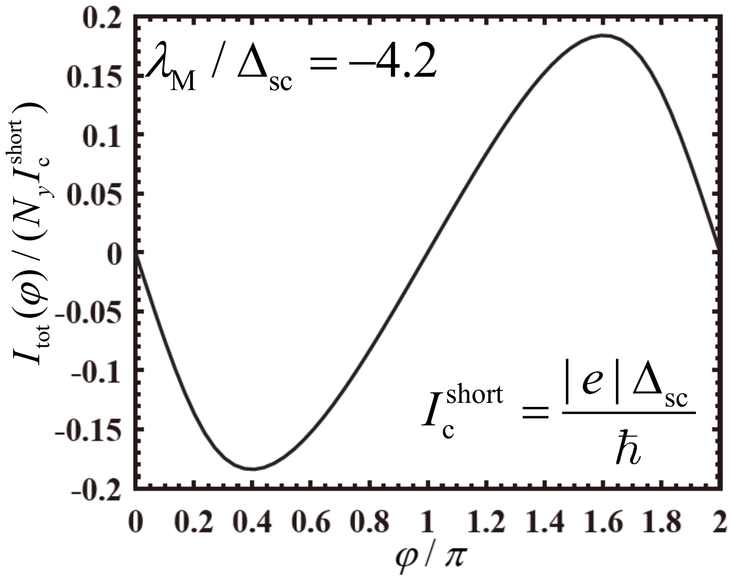

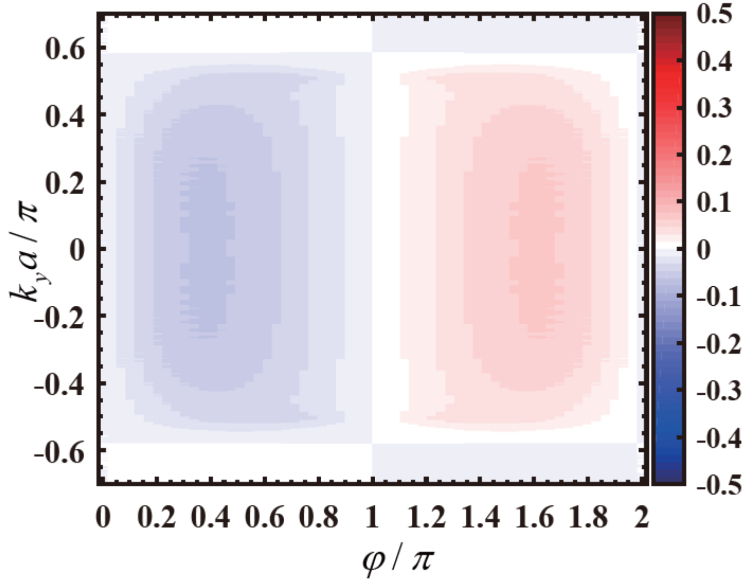

π - junction

The k_y dependent Josephson current density reveals additional features of the 0 - π transition

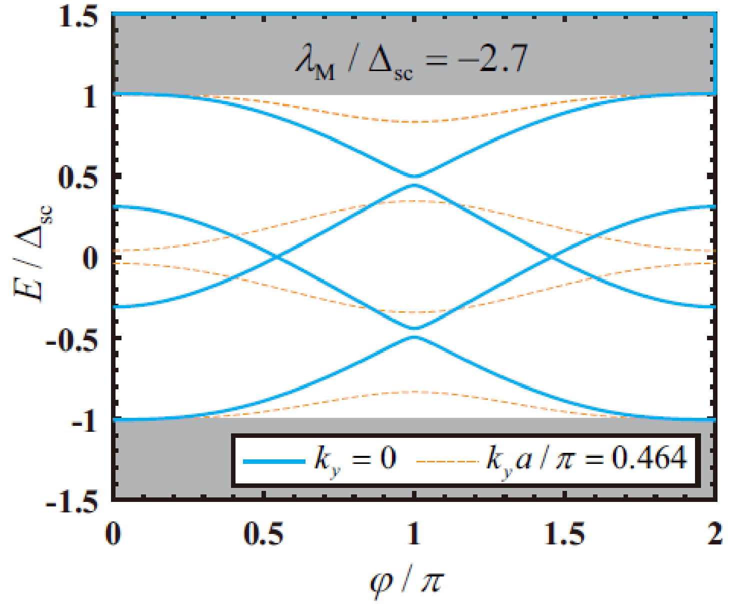

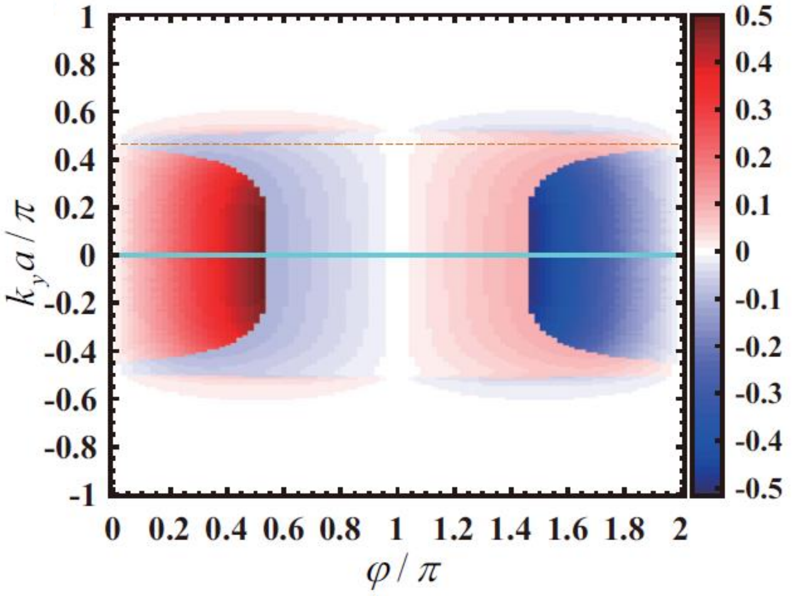

Coexistence of the 0 - junction and the π - junction behavior

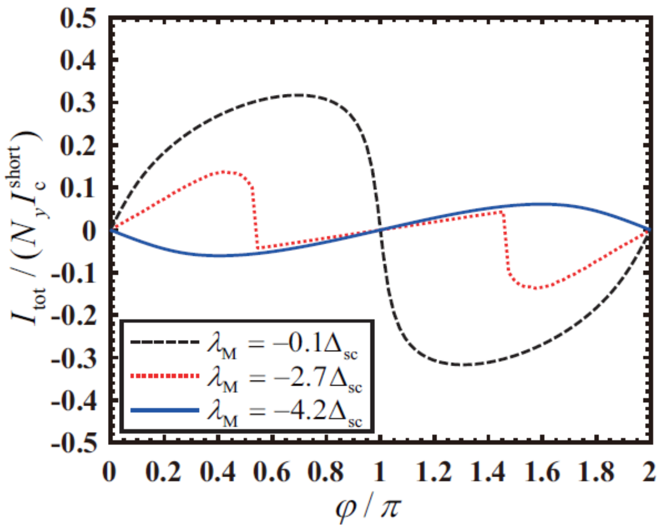

difference φ). As the total Josephson current is nevertheless still the superposition of many independent transverse channels, 0–π transitions in single k_y-channels do usually not yet facilitate a global 0–π transition of the whole 2DEG-based junction [87]. An experimental study of the transition regime

Costa *et.al.* 2023

Implications in experiments

Verification of the k_y dependent $0-\pi$ transition would request angular resolved Josephson current detection in 2D junctions

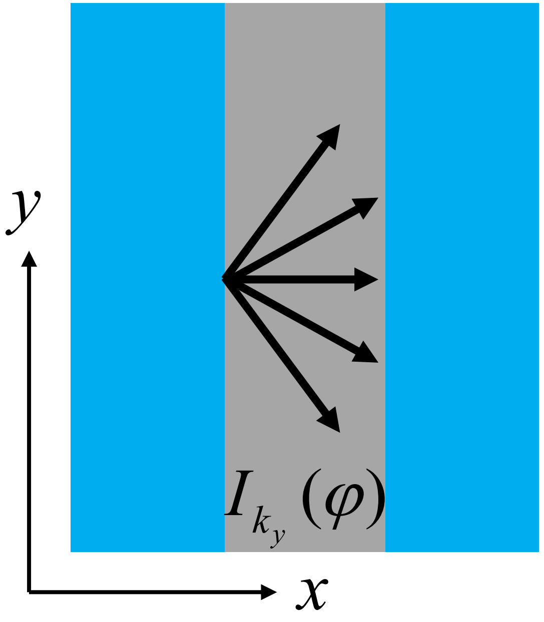

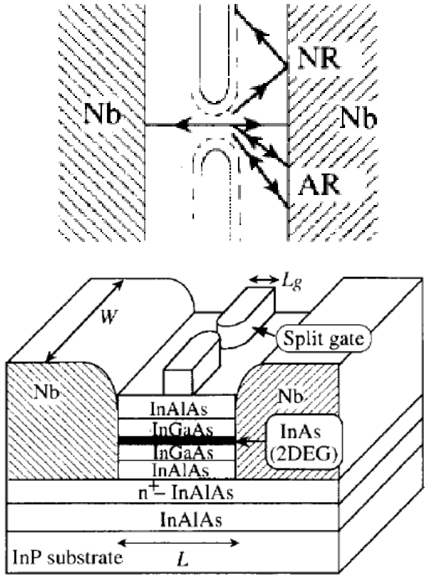

Takayanagi 1996

split gate electrode as a transverse momentum filter

Acknowledgement

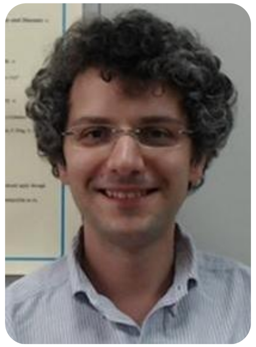

Seungju Han
Computational Science Research Center

Stefano Chesi
Computational Science Research Center

Mahn-Soo Choi
Korea University

Summary

Subgap modes in S/F/S junction with non-negligible lateral quasi-particle motion had been investigated

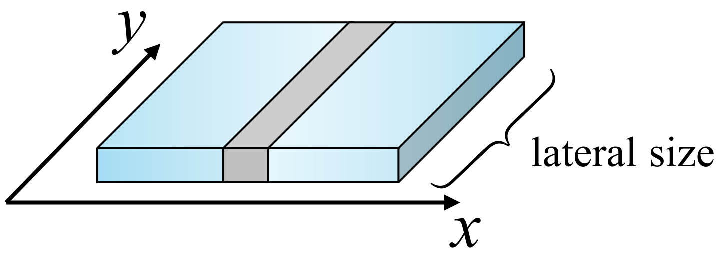

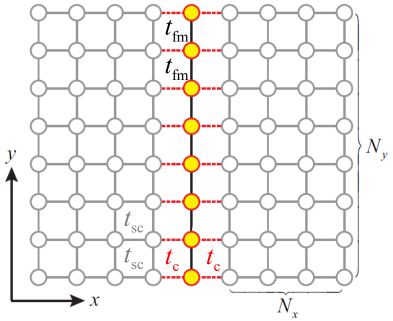

- Flat-dispersion
- Wave function
- $0-\pi$ transition

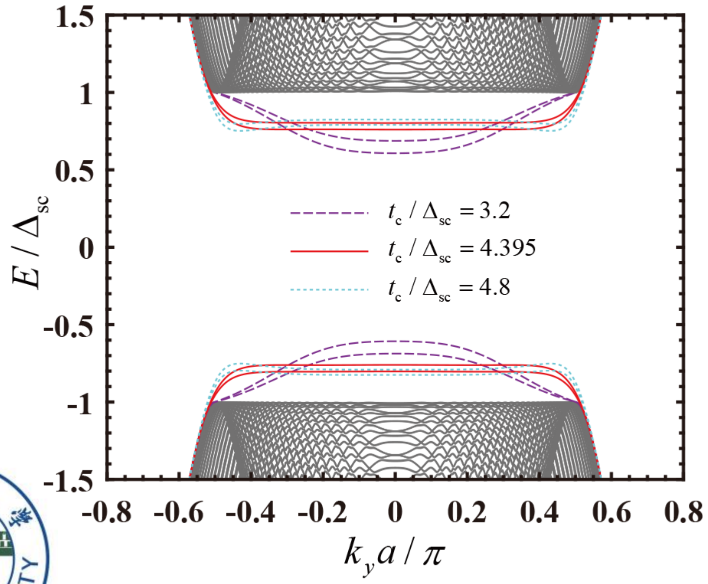

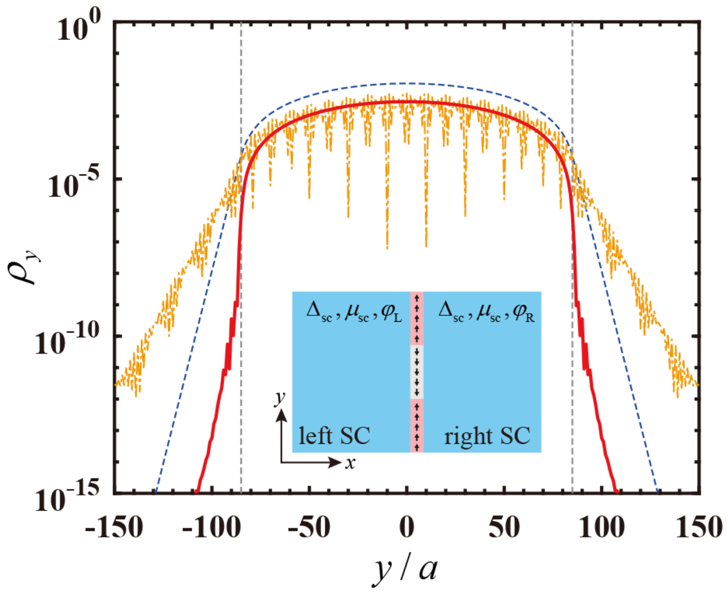

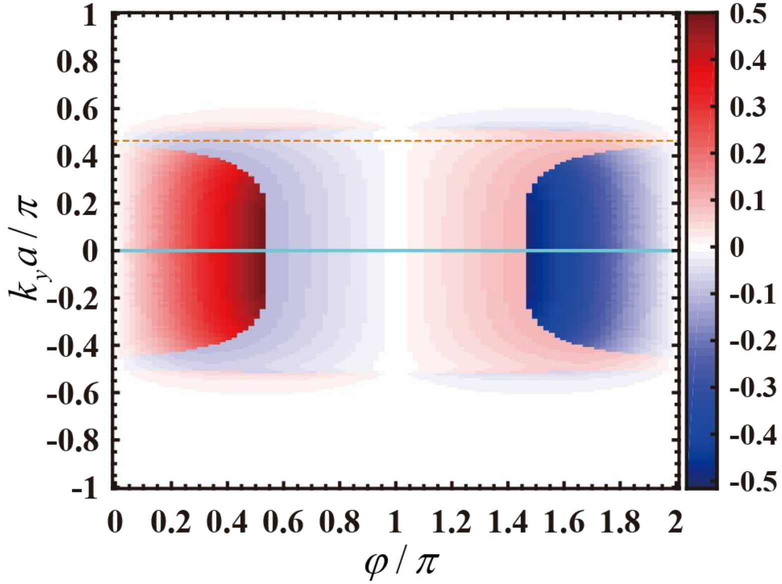

Thanks for your attentions!

Appendix: Typical parameters of the low T_c - superconductors

Tab. A.1.1 The critical temperature, London penetration depth, Ginzburg–Landau coherence length, critical fields and the energy gap of some superconductors.

Material	T_c [K]	λ_L [nm]	ξ [nm]	B_{c1} [T]	B_{c2} [T]	B_c [T]	2Δ [meV]
Nb	9.25	39	38	0.2	0.27	0.21	3.0
Pb	7.20	37	83	–	–	0.08	2.7
Al	1.18	16	1600	–	–	0.01	0.34
In	3.41	21	440	–	–	0.028	1.0
NbN	17.3	300	4		47	0.19[d]	6.4

Clarke and Braginski 2004

Appendix: Effects of magnetic fields

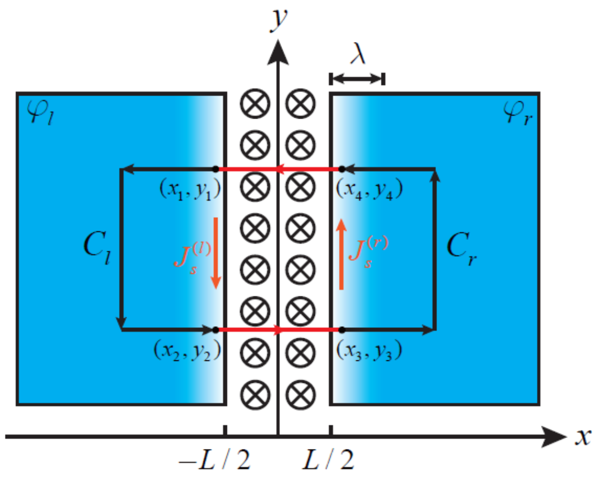

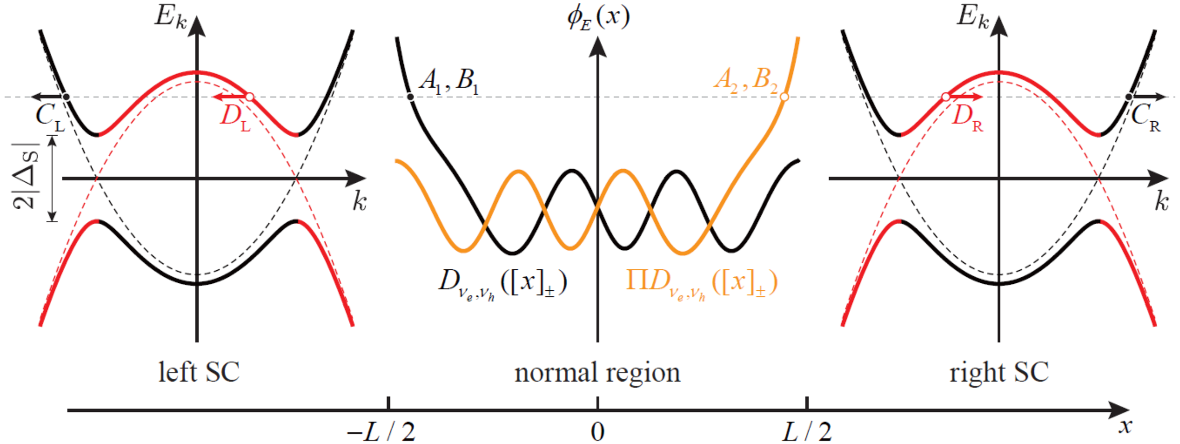

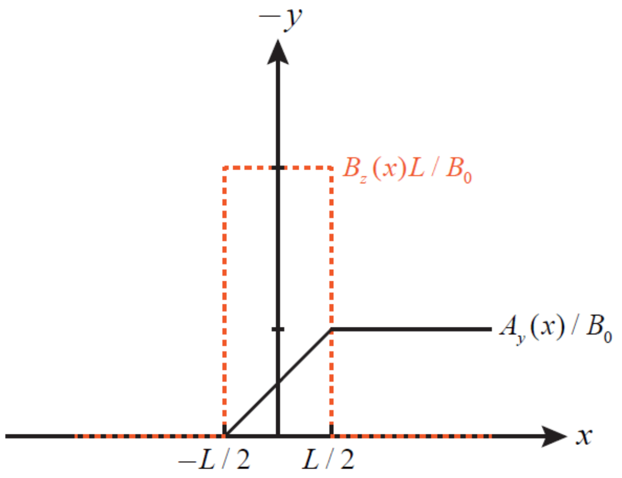

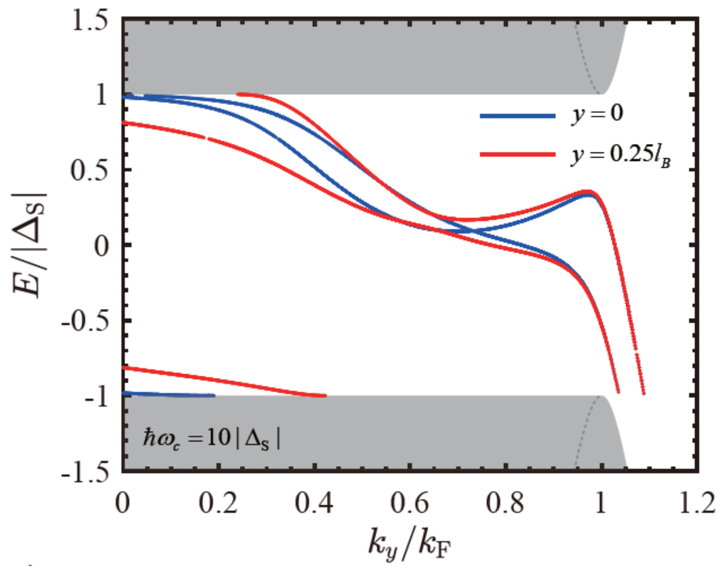

$$\varphi_L = \varphi_0 - \frac{1}{2}k_B y$$

$$\varphi_R = \varphi_0 + \frac{1}{2}k_B y$$

$$l_B = \sqrt{\frac{\hbar c}{eB_0}}$$